

UNIVERSITY OF HAWAII LIBRARY

CROSS-EQUATORIAL INTERACTIONS IN THE  
DEVELOPMENT OF A WINTER TYPHOON:  
NANCY 1970

A THESIS SUBMITTED TO THE GRADUATE DIVISION OF THE  
UNIVERSITY OF HAWAII IN PARTIAL FULFILLMENT  
OF THE REQUIREMENTS FOR THE DEGREE OF  
MASTER OF SCIENCE  
IN METEOROLOGY  
MAY 1974

By

Charles Philip Guard

Thesis Committee:

Colin S. Ramage, Chairman  
James C. Sadler  
Ronald C. Taylor

We certify that we have read this thesis and that in our opinion it is satisfactory in scope and quality as a thesis for the degree of Master of Science in Meteorology.

THESIS COMMITTEE

*C.S. Saurage*

Chairman

*James C. Sadler*

*Ronald C. Taylor*

TABLE OF CONTENTS

LIST OF TABLES . . . . . iv

LIST OF ILLUSTRATIONS . . . . . v

1.0. INTRODUCTION . . . . . 1

2.0. INVESTIGATIONS

2.1. Introduction . . . . . 8

2.2. Data and Analyses . . . . . 8

2.3. Results

2.3.1. Part I: February 1970 Prior to the  
Development of Typhoon Nancy . . . . . 11

2.3.2. Part II: The Development of  
Typhoon Nancy . . . . . 18

2.4. Summary and Conclusions . . . . . 36

3.0. SUGGESTIONS FOR FUTURE RESEARCH . . . . . 91

REFERENCES . . . . . 93

DATA SOURCES . . . . . 96

LIST OF TABLES

Table	Page
1 The mean 200 mb winds during February 1970 and the February long term 200 mb winds at Giles, Alice Springs, Cloncurry, and Noumea . . . . .	42
2 The gradient level winds for the period 10 through 17 February 1970 and the February long term mean gradient level winds at Port Moresby, Lae, Manus Island and Songkhla . . . . .	43
3 The 200 mb winds for the period 10 through 17 February 1970 and the February long term mean 200 mb winds at Koror, Truk and Ponape . . . . .	44
4 Surface pressure differences for the period 10 through 18 February 1970 and the February long term mean surface pressure differences for Hong Kong-Singapore, Hong Kong-Djakarta, Djakarta-Honiara, and Djakarta-Manus Island . . . . .	45
5 The five day mean geopotential heights for the periods 6 through 10 and 11 through 15 February 1970, the February 1970 mean geopotential heights, and the February long term mean geopotential heights at the 700 and 500 mb levels for Alice Springs, Darwin and Cloncurry . . . . .	46
6 Dew point depressions for a "normal" tropical sounding at Grand Bahama Island and for soundings at 00Z and 12Z on 16, 18 and 19 February 1970 at Truk Island . . . . .	47

LIST OF ILLUSTRATIONS

Figure		Page
1	Monthly variation in the average number of typhoons in the western North Pacific . . . . .	48
2	General analysis area for the study . . . . .	50
3	Departures of the mean February 1970 cloudiness from Sadler's February 6 year mean cloudiness . . . . .	52
4	250 mb streamline and isotach analysis for 00Z 16 February 1970 . . . . .	54
5	250 mb divergence pattern for 00Z 16 February 1970 . . . . .	55
6	ESSA 9 satellite mosaic photograph for 15 February 1970 . . . . .	56
7	ESSA 9 satellite mosaic photograph for 16 February 1970 . . . . .	57
8	Surface and gradient level streamline analysis for 00Z 16 February 1970 . . . . .	58
9	Truk time-section, indicating wind speed and direction, isohumes, $\theta_e$ , geopotential height differences, and position of the tropopause for the period 00Z 16 February 1970 through 00Z 20 February 1970 and 3 hourly surface observations for the period 18Z 15 February 1970 through 03Z 20 February 1970 . . . . .	60
10	Ponape time-section, indicating wind speed and direction, isohumes, $\theta_e$ , geopotential height differences, and position of the tropopause for the period 00Z 16 February 1970 through 12Z 19 February 1970 and 3 hourly surface observations from the period 18Z 15 February 1970 through 15Z 19 February 1970 . . . . .	62
11	ESSA 9 satellite orbital composite photograph for 16 February 1970 . . . . .	63

Figure	Page
12	Surface and gradient level streamline analysis for 00Z 17 February 1970 . . . . . 64
13	700 mb streamline and isotach analysis for 00Z 17 February 1970 . . . . . 65
14	500 mb streamline and isotach analysis for 00Z 17 February 1970 . . . . . 66
15	ESSA 9 satellite orbital composite photograph for 17 February 1970 . . . . . 67
16	250 mb streamline and isotach analysis for 00Z 17 February 1970 . . . . . 68
17	250 mb divergence pattern for 00Z 17 February 1970 . . . . . 69
18	Sea surface temperature analysis for February 1970 and the February long term mean sea surface temperature . . . . . 70
19	Surface and gradient level streamline analysis for 00Z 18 February 1970 . . . . . 71
20	ESSA 9 satellite orbital composite photograph for 18 February 1970 . . . . . 72
21	250 mb streamline and isotach analysis for 00Z 18 February 1970 . . . . . 73
22	700 mb streamline and isotach analysis for 00Z 18 February 1970 . . . . . 74
23	500 mb streamline and isotach analysis for 00Z 18 February 1970 . . . . . 75
24	250 mb divergence pattern for 00Z 18 February 1970 . . . . . 76
25	Surface and gradient level streamline analysis for 00Z 19 February 1970 . . . . . 77
26	250 mb streamline and isotach analysis for 00Z 19 February 1970 . . . . . 78
27	ESSA 9 satellite orbital composite photograph for 19 February 1970 . . . . . 79

Figure	Page
28 250 mb divergence pattern for 00Z 19 February 1970 . . . . .	80
29 Surface and gradient level streamline analysis for 12Z 19 February 1970 . . . . .	81
30 700 mb streamline and isotach analysis for 12Z 19 February 1970 . . . . .	82
31 500 mb streamline and isotach analysis for 12Z 19 February 1970 . . . . .	83
32 250 mb streamline and isotach analysis for 12Z 19 February 1970 . . . . .	84
33 250 mb divergence pattern for 12Z 19 February 1970 . . . . .	85
34 Surface and gradient level streamline analysis for 00Z 20 February 1970 . . . . .	86
35 ESSA 9 satellite mosaic photograph for 20 February 1970 . . . . .	87
36 250 mb streamline and isotach analysis for 00Z 20 February 1970 . . . . .	88
37 ESSA 9 satellite mosaic photograph for 21 February 1970 . . . . .	89
38 250 mb divergence pattern for 00Z 20 February 1970 . . . . .	90

CROSS-EQUATORIAL INTERACTIONS IN THE DEVELOPMENT  
OF A WINTER TYPHOON: NANCY 1970

1.0. INTRODUCTION

One area of meteorological research which has been badly neglected is that of tropical cyclones that occur during winter--"off-season typhoons."<sup>1</sup> Although rare, these tropical cyclones are just as intense and devastating as those that occur during the normal typhoon season. Typhoon Opal, December 1964, attained maximum intensity of 170 knots and a minimum surface pressure of 903 millibars. Typhoon Kit, January 1972, produced surface winds of 120 knots and left in her wake, 204 persons dead and property damage near 23 million dollars (U.S.). Typhoon Nancy, February 1970, attained surface winds of 120 knots, a minimum surface pressure of 949 millibars and rendered 5,000 persons homeless as she paralleled the eastern coast of the Philippine Islands.

"Off-season typhoons" are most common in the western North Pacific, but Gibbs (1956) refers to their occurrence in the region of Australia as well. Figure 1 shows that the number of typhoons from December through April, in the western North Pacific, is only about 8% of those occurring

---

<sup>1</sup>"Off-season typhoons" refer to tropical cyclones which occur from December through April in the Northern Hemisphere.



during the remaining months. February exhibits the smallest frequency, with one typhoon about every 13 years, although prior to Typhoon Nancy, the last February typhoon occurrence was Typhoon Irma, February 1953.

Since there have been few, if any, studies involving "off-season typhoons", one can pose the question: how do they differ from other typhoons? It seems plausible to assume that the structure and mechanics of mature tropical cyclones are similar, regardless of season. We therefore postulate that the primary difference between winter and the other seasons arises from changes in the general circulation, which in turn alters the thermal and dynamical characteristics of the air, and probably the mixed layer of the underlying ocean. It therefore seems likely that a fundamental difference between "off-season typhoons" and "seasonal" ones is in their formation, which, in turn arises from changes in the general circulation itself. Thus we pose the following question: how do "off-season typhoons" differ from "seasonal" ones in their formation and development?

Several authors [Palmén (1956), Riehl (1954), Wilkie (1964), and Palmén and Newton (1969)], have listed a number of necessary conditions for the formation of tropical cyclones. The most important are: (1) large sea areas with a water temperature so high (above 26 or 27°C.) that when moist air, with nearly this temperature, is lifted

from the lowest layers of the atmosphere and expanded pseudo-adiabatically, it remains considerably warmer than the environment, at least to 12 km; (2) weak vertical wind shear in the basic wind field; (3) a minimum value of the Coriolis parameter, requiring development poleward of 5 to 8° latitude; (4) a pre-existing, low level disturbance; and (5) upper tropospheric outflow above the region of development.

Mechanisms to explain the formation of a pre-existing, low level disturbance were devised by Riehl (1945) in his easterly wave theory and by Palmer (1951) in his equatorial wave hypothesis. Sadler (1967) has been critical of these theories and insists that "all tropical vortices form initially in a shear zone between two currents of opposite direction." In the western Pacific, during the Northern Hemisphere winter, low level westerlies are generally south of the equator, while easterlies dominate to the north. If Sadler is correct, we must expect a considerable alteration of the general, low level circulation during the formation of "off-season typhoons."

Two different ideas have developed involving the upper tropospheric outflow above the region of development: one asserts the significance of an internally generated mechanism, the other of an externally imposed one. Gray (1968) argues that cyclogenesis is induced within the disturbance with upper tropospheric outflow being created

(through the Durst-Sutcliffe effect<sup>2</sup>) by the disturbance itself, with the primary requirement being one of sufficient, low level convergence. In contrast to the above, others [Riehl (1948), McRae (1956), Ramage (1959), and Palmén and Newton (1969)], argue that upper level divergence is associated with upper tropospheric mid-latitude troughs which penetrate into the tropics. Namias (1955) indicates that when mid-latitude waves move into tropical regions, they may act to hydrostatically destabilize the tropical troposphere and intensify low level disturbances. Ramage (1973) cites three cases in which typhoons exhibited intensification when under areas of strong, upper level divergence to the east of upper tropospheric troughs. McRae (1956) notes that in the region of Australia, when a jet stream intensifies in the subtropics during summer, the cause is usually the result of increasing amplitude of a long wave trough in the upper troposphere. He also found that when 200 mb divergence was located on the warm side of the jet axis (where velocity and anticyclonic curvature and shear increased downstream), it was almost invariably associated with tropical cyclogenesis, when the divergence occurred over

---

<sup>2</sup>Durst and Sutcliffe (1938) showed that with upward motion in a region of horizontal temperature gradient, there is a component of motion directed towards the cooler air, thus the association of the ascending air and a warm core will result in divergence.

the ocean. Koteswaram and George (1957) conclude that tropical cyclogenesis in the Bay of Bengal occurs in association with upper tropospheric divergence produced by the passage of an upper level ridge over a low level cyclonic vortex. Finally, Ramage (1973) and Burroughs (1974) have indicated that divergence of heat flux may play an important role in the intensification of tropical cyclones.

During the Northern Hemisphere winter the upper tropospheric subtropical ridge is located near  $12^{\circ}\text{N}$ ; hence, tropical cyclogenesis must occur relatively close to the equator. This suggests that transequatorial interactions of the circulation might be involved in the formation and development of "off-season typhoons." From December to April the low level flow in the tropics of the western Pacific is generally northeasterly north of the equator. Crossing the equator, the winds turn counterclockwise producing the northwest monsoon of Australia and Indonesia, with accompanying widespread ascending motion (Deppermann, 1941). Concurrently, no near-equatorial trough appears to exist in the Northern Hemisphere. Of the monsoon regions, Ramage (1971) describes two contrasting precipitation regimes: (1) "rains" and (2) "showers." "Rains" are characterized by "deep nimbostratus embedded with cumulonimbus in an area where vertical wind shear and lower tropospheric convergence are large." "Showers" are

characterized by "scattered towering cumulus or cumulonimbus in an area where vertical wind shear and lower tropospheric convergence are small." During the Northern Hemisphere winter, the portion of Indonesia lying south of the equator is normally dominated by the "rains" regime.

Ramage (1971) asserts that "as the vertical plane circulation of a monsoon system or a transequatorial Hadley cell intensifies, associated surface winds equatorward of a near-equatorial trough freshen and cause a local increase of cyclonic vorticity in the trough." Perhaps such intensifications could play a role in the formation and development of "off-season typhoons."

The purpose of this study is to examine the formation and development of a winter typhoon (Typhoon Nancy: February 1970) and to determine whether significant differences exist between her formation and development and that of "seasonal" typhoons. Particular attention is given to the role of cross-equatorial interactions.

February 1970 was anomalous in both its circulation and its weather distribution, at least in the tropical and subtropical regions between  $90^{\circ}\text{E}$  and  $180^{\circ}$ . An understanding of the circulation in this region during that part of February prior to the formative stages of Nancy was essential in understanding the cross-equatorial interactions that occurred during her formation and development. Accordingly, the investigation was performed in two parts:

Part I, which is descriptive and concerns that part of February 1970 prior to the 16th, examines the salient circulation anomalies and utilizes them to explain the resulting circulation and weather distributions in the tropics of both hemispheres. Part II, which is synoptic and dynamical, covers the period (16-20 February) leading up to and including the formation of a tropical depression and its subsequent development into the mature tropical storm, Nancy.

## 2.0. INVESTIGATIONS

### 2.1. Introduction

Why was Nancy chosen? She occurred during the Northern Hemisphere winter when the Australian and Indonesian northwest monsoon is normally well developed. She developed into a tropical storm near Truk Island and intensified into a strong typhoon over Yap Island, both locations from which rawinsonde data is available. Her minimum sea level pressure dipped to 949 millibars and her maximum wind speed reached 120 knots. Finally, Nancy occurred during a period when aerological conditions deviated considerably from the mean. This should facilitate delimiting some of the conditions responsible for the formation and development of Nancy.

### 2.2. Data and Analyses

Data for the study was taken from numerous sources which are listed in the Data Sources section. When possible, corrected data sources were used, although this was not always possible for stations in the Southern Hemisphere. The Northern Hemisphere upper air data was taken from the National Weather Service (NWS) Northern Hemisphere Data Collection, except for Japan and Korea where the Japan Meteorological Agency (JMA) Aerological Data of Japan was used. Since most stations in The Peoples' Republic of China do not report the 250 mb level,

it was obtained by interpolation between the 200 and 300 mb levels. The interpolation was checked with two stations in China that do report the 250 mb level and was found satisfactory. Since over the western North Pacific, there are few rawinsonde stations, Fleet Numerical Weather Central Pearl Harbor "plotreps" aircraft data was used where upper air data was sparse or missing. This produced nearly a ten fold increase in the 250 mb data over this area.

Surface data was primarily obtained from synoptic data tabulations in the Daily Weather Maps of the JMA. In order to augment this data, the NWS Northern Hemisphere Data Collection was utilized. Copies of the original surface weather observations (WBAN Form 10A) were used for stations in the Caroline and Marianas Islands.

Data for the Southern Hemisphere, both surface and upper air, was taken from the Daily Weather Bulletins of the New Zealand Meteorological Service (NZMS) and from the daily weather maps of the Regional Meteorological Center (RMC), Darwin. Environmental Technical Applications Center surface weather data was used for Indonesia, the Philippines, and Southeast Asia.

The area of interest (Figure 2) was chosen to include the subtropical ridges of each hemisphere in its north-south extent and the northwest monsoon in the east-west direction. All wind speeds are given in knots.



When mean values are discussed, they have been taken from the Meteorological Atlas of the International Indian Ocean Expedition (Ramage and Raman, 1972), from The Mean Winds of the Upper Troposphere over the Central and Eastern Pacific (Sadler, 1972), and from the ESSA World Weather Records.

Upper air analyses were performed at the 700, 500, 300, and 250 mb levels. They were prepared using 00Z data, except that on 19 February, both 00Z and 12Z analyses were made. Surface analyses were prepared for 00Z and 12Z from 00Z 16 February through 00Z 20 February. Gradient level winds were utilized in the tropical and subtropical regions where baroclinity was small.

In the discussion of February 1970, prior to the development of Typhoon Nancy, the primary data sources were ESSA 9 satellite mosaics and upper air and surface analyses prepared by RMC, Darwin.

The time cross-sections of Truk Island and Ponape Island were prepared using data from the NWS Northern Hemisphere Data Collections. The computation of  $\theta_e$  was performed using a computer program, THETA E (Burroughs, 1974). Soundings were reconstructed where data was questionable and the time-sections were checked to insure hydrostatic consistency. Geopotential height changes were obtained as the difference between successive 24 hour height values. Values for Truk at 12Z on the 18th, above

the 405 mb level, were obtained by interpolation between the respective preceding and succeeding observations.

The dynamical study consisted of computing the divergence, vorticity, and kinetic energy (KE) at the 250 mb level over selected areas of the western Pacific. This was accomplished with a computer program (Murakami and Sadler, 1973). Wind speed and direction were extracted at 2° grid intervals in the region of interest and all calculations were based on this data. It is evident that the dynamical results are entirely dependent on the 250 mb analyses. All references to divergence, vorticity and kinetic energy in Part II will pertain to values at the 250 mb level, unless stated to the contrary.

The ESSA 9 satellite pictures (mosaics and orbital composites) were invaluable in augmenting lower and upper level wind data and in displaying the day to day changes in the distribution of weather.

### 2.3. Results

#### 2.3.1. Part I: February 1970 Prior to the Development of Typhoon Nancy

About 8 February 1970, the Southern Hemisphere near-equatorial trough (NET) west of Australia became very active and produced over a three day period, four tropical cyclones. The following day the NET east of Australia also became very active and generated three tropical cyclones in

a two day period. Six of these tropical circulations can be seen in the ESSA 9 satellite mosaic for 15 February in Figure 6. The reasons for the prolific tropical cyclone development are undoubtedly complex, but certain patterns give us insight into the problem.

Wind observations at the 200 mb level at Giles, Alice Springs, Cloncurry and Noumea are shown in Table 1. The mean February 1970 winds at Giles, Alice Springs, and Cloncurry all possess a more southerly component than indicated by the long term mean. This implies much deeper than normal trough penetrations from the mid-latitudes. Noumea 200 mb winds are 15 knots stronger than the long term mean. For ten days prior to the sudden onset of tropical cyclone development east of Australia, Noumea 200 mb winds were in excess of 65 knots and exceeded 80 knots during half this period. On the 9th, winds at Cloncurry and Alice Springs were 25 and 10 knots respectively, while those at Noumea were 85 knots. This suggests a strongly divergent circulation between eastern Australia and the New Hebrides Islands. Gibbs (1956) described conditions preceding the development of a tropical cyclone in the Gulf of Carpentaria. There was, at 200 mb, a slow moving anticyclone east of a deep, but retrograding trough oriented NW-SE south of the Gulf. He further spoke of a strong jet stream at 25°S. McRae (1956) observed that "intensification usually occurs beneath a region of

divergence on the warm side of the subtropical jet axis. The divergence results from the increasing amplitude of a long wave trough." These conditions described by Gibbs and McRae appear nearly identical to those observed east of Australia in early February 1970 during tropical cyclone development. One can visualize a similar deep penetrating trough upstream, over the Indian Ocean, producing the same effects west of Australia on the preceding day.

After the tropical cyclones formed east of Australia, the gradient level winds at Lae and Port Moresby accelerated to 50 knots. Upper level, southeasterly winds accelerated on the 11th over an area from Koror to Ponape and lower level northwesterly winds accelerated over New Guinea on the 12th (see Tables 2 and 3). Upper level winds again exhibited maximum acceleration on the 16th and low level northwesterly winds at Manus Island exhibited their maximum acceleration on the 17th. Thus, it appears that large upper tropospheric accelerations from a southeasterly quarter just north of the equator, proceed low level, northwesterly accelerations just south of the equator. The low level response seems to lag the upper level accelerations by about a day and appear to be confined to a much smaller area than are the upper level accelerations. During the strong, upper tropospheric accelerations, the maximum wind speeds occurred between the 125 and 175 mb levels. A survey of the January and

February upper level winds from 1965 to 1972 showed that strong accelerations occur on the average, once or twice a month over the Caroline Islands and somewhat more frequently over the western Marianas Islands. They are generally strongest between Koror and Ponape, the area where most off-season typhoons develop. These accelerations seem generally to be associated with an increase in cloudiness over the Carolines, but not necessarily over the western Marianas.

Table 4 shows the surface pressure differences between selected Northern Hemisphere stations and Southern Hemisphere stations. The Northern Hemisphere stations are generally beneath upper tropospheric convergence, while those to the south are generally beneath upper tropospheric divergence. The Hong Kong-Singapore and Hong Kong-Djakarta surface pressure differences were greatest when the greatest upper tropospheric wind speeds were observed over Koror, but also exhibited a maximum when strong accelerations occurred over Truk and Ponape. Simultaneous with these pressure differences, were moderate surges in the South China Sea and gradient level winds in excess of 35 knots at Songkhla (see Tables 2 and 3). Singapore-Honiara surface pressure differences were greatest when low level wind speeds were greatest over New Guinea, but strong east-west surface pressure gradients were not observed with the strong low level wind accelerations over Manus Island.

We may assume that strong upper tropospheric divergence is occurring to the east and west of Australia, where tropical cyclogenesis is occurring. In response, strong upper level convergence should exist over central Australia, which would weaken the surface heat low. Just prior to and during the early period of cyclone development near Australia, surface pressures over central Australia did rise. However, by 10 February, the surface pressures began to fall and continued to do so for a number of days. This could occur from increased upper tropospheric divergence in the vicinity of the tropical cyclogenesis, which would in turn increase the upper level convergence over Australia; the consequent increased subsidence would reduce the surface pressures. Ramage (1971) illustrates an inverse relationship between the intensity of the monsoon rains over India and the intensity of the West Pakistan heat low. Perhaps the rising surface pressure over Australia is a result of increased upstream, upper level convergence induced by the heavy precipitation associated with the tropical cyclones near Australia. A look at the 700 and 500 mb geopotential heights at selected stations over Australia gives some insight into what happened (see Table 5). Five day means indicate that the geopotential heights were below or near normal prior to and during the early stages of tropical cyclone development. Five day means from the 10th through the 14th show

a significant elevation of these height surfaces. Since the thickness between isobaric surfaces is proportional to the mean virtual temperature, there must be warming in the lower and middle troposphere. There is no apparent advection of warm air into the region, so we must conclude that the warming was a result of adiabatic expansion from strong subsidence. This prevented further surface pressure rises. Subsidence would hinder cloud formation, which would in turn, increase insolation, surface temperatures and intensify the surface heat low. Thus, a feedback mechanism was set up that produced fine weather over Australia. Figure 3 shows that central and northern Australia was less cloudy than normal.

Prior to the copious Southern Hemisphere tropical cyclogenesis east of Australia, cloudiness over Indonesia was profuse. ESSA 9 satellite mosaics indicate strong convective activity, which is characteristic of the northwest monsoon. The counterclockwise curving "cross-equatorial drift,"<sup>3</sup> supplying low level convergence, coupled with divergent upper tropospheric flow, is responsible (Ramage, 1971). The upward branch of the Hadley cell transports the released heat energy to the mid-latitude westerlies in the Northern Hemisphere.

---

<sup>3</sup> Johnson and Mörth (1960) labelled cross-equatorial flow from high pressure to low pressure as "cross-equatorial drift."

From the 13th through the 16th of February, the vigorous convection over Indonesia slowly subsided and did not recur until the end of February, after Typhoon Nancy had moved into the mid-latitude westerlies. Whether or not the presence of Nancy played a part in prolonging the "showers" regime over Indonesia is not clear, but Sutrisno (1963) notes that tropical cyclones in the western North Pacific (not "off-season typhoons") and in the Bay of Bengal do significantly affect the rainfall in the southwestern part of Indonesia. What reduced convection over Indonesia? Two reasons come to mind. First, the surface circulation began to change prior to the 16th, in such a way as to reduce low level convergence over Indonesia. This alteration of the low level flow will be elaborated on in Part II. Secondly, the upper level divergent winds appear to have been replaced by weakly convergent winds, a result of acceleration of the upper level winds east of Indonesia and a deceleration of these winds west of Indonesia.

Figure 3 shows that during February 1970, the Indonesian Archipelago experienced significantly less cloudiness than is indicated by the six year mean. It is interesting to note that as the convective activity over Indonesia was subsiding, a new area of vigorous convection was forming to the east of the Solomon Islands, near the equator. Looking again at Figure 3, we find that the area



to the east of the Solomon Islands possessed substantially more cloudiness than is usual. The central North Pacific also possessed above normal cloudiness. It appears that in the latter half of February 1970, a drastic change took place in the mean circulation. The mean meridional or Hadley circulation appears overshadowed by the mean zonal circulation. The excessive cloudiness in the central North Pacific is a reflection of a marked weakening in the subsiding branch of the Hadley cell. Figure 3 indicates that the zonal circulation was strongest just south of the equator, with its rising branch to the east of the Solomon Islands and its descending branch over Indonesia. During the last half of February 1970, the "showers" regime over Indonesia prevailed, but the area to the east of the Solomon Islands exhibited frequent fluctuations in cloudiness. This suggests that perhaps the zonal circulation spanned a much broader area, with its upward branch located, at least some of the time, east of the dateline as described by Walker (1923).

#### 2.3.2. Part II: The Development of Typhoon Nancy

Between 00Z on the 15th and 00Z on the 16th, the upper tropospheric winds at Funafuti ( $08^{\circ}31'S$ ,  $179^{\circ}12'E$ ) and Pago Pago ( $14^{\circ}20'S$ ,  $170^{\circ}43'W$ ) slightly decelerated, while those over the Marshall and Caroline Islands exhibited large accelerations, creating a strongly divergent upper tropospheric flow between Funafuti and the

Caroline Islands (Figure 4). The 250 mb winds at Ponape changed from  $138^\circ$  at 10 knots to  $145^\circ$  at 54 knots during this period. The 00Z 16 February divergence analysis verifies the strongly divergent flow in this region with a maximum value of  $2.8 \times 10^{-5} \text{ sec}^{-1}$  at  $5^\circ\text{N}$ ,  $159^\circ\text{E}$  (Figure 5). The vorticity patterns indicate weak positive vorticity to the west of the region of maximum divergence, but strong negative vorticity, in excess of  $4 \times 10^{-4} \text{ sec}^{-1}$  to the east. The kinetic energy (KE) in the area of maximum divergence is greatest at  $6^\circ\text{N}$ ,  $160^\circ\text{E}$  and exceeds  $240 \text{ m}^2 \text{ sec}^{-2}$ .

The ESSA 9 satellite pictures (Figures 6 and 7) indicate vigorous convection in this region, a condition which markedly increased from the 15th to the 16th. Possibly redistribution of heat of condensation was responsible for the strong accelerations, but the abruptness and intensity of the changes suggest an additional impetus. Perhaps it was from the Northern Hemisphere where the jet stream exceeded 200 knots. Or perhaps, it was from the Southern Hemisphere where the Tropical Upper Tropospheric Trough (TUTT) was extremely strong. Winds at the 250 mb level at Penrhyn Island ( $09^\circ 01'\text{S}$ ,  $158^\circ 04'\text{W}$ ) were  $170^\circ$  at 55 knots and at Rarotonga Island ( $21^\circ 12'\text{S}$ ,  $159^\circ 46'\text{W}$ ) were  $170^\circ$  at 50 knots. For the respective stations, the mean 250 mb winds for February are  $200^\circ$  at 15 knots and  $260^\circ$  at 10 knots. It seems feasible that

energy interactions between the two strong circulations might have been responsible. The Northern Hemisphere 250 mb ridge was dominated by a massive anticyclone, centered near Eniwetok Atoll, which encompassed the entire Northern Hemisphere tropics from Southeast Asia to 170°W.

The surface analysis of the 16th (Figure 8) shows China dominated by a surface anticyclone, from which a moderate surge emanated. Ship observations in the South China Sea indicate northeasterly wind accelerations of 20 knots from the 15th to the 16th, while the gradient level winds at Songkhla increased from 10 knots to 35 knots during this period. The accelerations occurred simultaneously with the large upper level wind accelerations and the large Northern Hemisphere-Southern Hemisphere pressure gradients discussed in Part I (see Tables 2 and 3).

The normal "cross-equatorial drift" which usually recurves near the equator, was displaced northward, creating a surface trough in the Northern Hemisphere and winds with a westerly component along the equator. The gradient level winds at Manus Island were northwesterly at 40 knots while the northeast trades were 20 to 30 knots over the Caroline Islands. The potential for the generation of positive vorticity was created in the shear zone south of the Caroline Islands.

The time cross-sections of Truk and Ponape (Figures 9 and 10) indicate that a rapid and deep invasion of moisture

arrived at Ponape prior to its arrival at Truk. Rain began at Ponape 15 hours before it began at Truk. By 12Z on the 16th, the 75 percent isohume was above the 400 mb level at Ponape and above the 300 mb level at Truk. Table 6 shows that the atmospheric column over Truk was considerably more moist at 12Z than at 00Z, especially in the middle troposphere. The 12Z sounding shows that the column was saturated between 565 and 400 millibars. The effects of this moisture will be discussed later.

At Ponape, large geopotential height falls occurred throughout the upper and middle troposphere, falling more slowly at 12Z. Smaller geopotential height falls at Truk lagged those at Ponape by about 12 hours. The geopotential height falls suggest that if an area of lower surface pressure were to form that it would do so somewhat closer to Ponape than Truk. This information and that of the divergence and KE analyses support the placement of the initial surface low at about  $4.5^{\circ}\text{N}$ ,  $160^{\circ}\text{E}$ , corresponding to a relatively clear area in the region of intense convection (Figure 11).

The 00Z 17 February surface analysis (Figure 12) shows that the anticyclone over China moved northeastward to the China coast, while the surge in the South China Sea began to weaken. The surface and gradient level flow in the tropics changed drastically as the normal "cross-equatorial drift" into central and eastern Indonesia was interrupted

by the continued northward movement of the near-equatorial trough (NET) in the Northern Hemisphere. Two cyclonic vorticies were prominent in the trough, one near Koror Island and one at  $5^{\circ}\text{N}$ ,  $155^{\circ}\text{E}$ . The former vortex, not associated with any organized cloudiness, persisted through the 19th, but showed no warm core characteristics. On the 19th, it moved northeastward as part of a low level, extra-tropical trough. The latter vortex was destined to become Typhoon Nancy.

On the 17th, low level flow north of the Northern Hemisphere NET remained 20 to 30 knots, being 40 knots at Truk. To the south, Manus Island exhibited northwesterly winds of 50 knots and a ship reported 20 knot westerly winds at  $3^{\circ}\text{N}$ ,  $152^{\circ}\text{E}$ . Consequently, a zone of strong shear resulted.

The flow at the 700 mb level (Figure 13) places the Southern Hemisphere ridge line  $8^{\circ}$  north of its normal position. The westward extent of the outflow to the north of the anticyclone was  $10^{\circ}$  east of its normal westward range and the recurvature of this flow into westerly winds was more equatorward than normal. These departures of the 700 mb circulation produced slightly divergent flow over southern Indonesia, enhancing fine weather and contributed to a further weakening of the Southern Hemisphere NET. In spite of 50 knot westerly winds at Manus Island and 40 knot easterly winds at Truk at the 700 mb level, no cyclonic

vortex was yet apparent at this level over the Caroline Islands.

At 500 millibars on the 17th, a large anticyclone over Australia, produced strong equatorward outflow (Figure 14). Most of the outflow recurved into northwesterly flow which entered tropical cyclone Dawn east of Australia. The remaining outflow was diverted across the equator into a small cyclonic vortex over the Caroline Islands.

The ESSA 9 satellite photograph (Figure 15) indicates an increase in anticyclonic outflow at the cirrus level over and to the north of the Caroline Islands. The 250 mb analysis (Figure 16) places a mid-latitude trough near the Philippine Islands reducing the westward extent of the large anticyclone over the western Pacific. At 250 millibars, the divergence above the low level vortex was  $1.7 \times 10^{-5} \text{ sec}^{-1}$ . The large gradient in the divergence pattern (Figure 17), west of the surface vortex is dubious and probably results from a poor analysis of the speed field in this data-sparse area. The vorticity analysis indicates positive vorticity to the south and west of the low level circulation, but the vortex is beneath negative vorticity of  $9 \times 10^{-5} \text{ sec}^{-1}$ . The remaining area north of the equator, exhibits strong negative vorticity, at least to  $26^\circ\text{N}$ . The KE above the vortex is  $148 \text{ m}^2 \text{ sec}^{-2}$ , nearly a 40% decrease from that on the 16th.

The Truk and Ponape time sections (Figures 9 and 10)

show a substantial decrease in the upper level wind speed, although Ponape has retained winds in excess of 50 knots at the 100 mb level. The deceleration was probably a result of the prolific convection.

Why did a near-equatorial trough form in the Northern Hemisphere during February 1970 and why was it so persistent? It appears that the distribution of the sea surface temperature (SST) may have played an important role in the persistence and anchoring of the Northern Hemisphere NET. An analysis of the February 1970 SST (Figure 18) indicates that the SST was from 1° to 2°C warmer than normal in the Northern Hemisphere tropical regions. The sea surface isotherms indicate a maximum from near 4°N southwest of Truk, westward to 4°N, 138°E and northward to 10°N near Yap Island. It is not clear why the SST was higher than normal or why a maximum was located north of the equator during February 1970. Ramage (1974) has evidence that near-equatorial troughs are thermally anchored, therefore, it seems plausible to assume that a weak surface trough (in the pressure field) would have existed over the region of the maximum sea surface temperatures during February 1970. The strong, divergent, upper level winds induced wide-spread convection in the area. Where divergence aloft was greatest, a region or regions of lower relative surface pressure were created in the locale of the convection. The question arises whether

or not other factors could have contributed to the reduction of the surface pressure. It seems apparent that the rapid influx of less dense, moist air could reduce the hydrostatic pressure. Bhumralkar (1974) showed that a moist column of air would create a surface pressure more than 2 millibars lower than the same column of dry air. He used a "normal" sounding at Grand Bahama Island which is similar to the sounding at Truk at 00Z on the 16th (see Table 6). Table 6 shows that the atmospheric column over Truk at 12Z on the 16th is considerably more moist at all levels than at 00Z; consequently, the hydrostatic pressure would decrease from 00Z to 12Z on the 16th. Bhumralkar further showed that the presence of condensed water in the column of moist air would increase the surface pressure by about 1 millibar, thus resulting in an overall surface pressure more than 1 millibar lower than if the column were dry. The influx of moisture indicated at Truk and Ponape (Figures 9 and 10) from 00Z to 12Z on the 16th would contribute to a lowering of the surface pressure in the entire region, but since the area of lowest pressure was located in a relatively clear area, the corresponding increase of the hydrostatic pressure due to condensed water in the column would be much smaller than in the surrounding area where convection is profuse. This would increase the surface pressure gradient and further intensify the surface trough. Since tropical disturbances



and tropical depressions exhibit small pressure gradients, the hydrostatic effect of moisture could be important in their formation. The strong, low level westerly winds south of the equator expanded the realm of westerlies from their normal domain to north of the equator. These winds, coupled with the strong, northeasterly trade winds over the Carolines, created an area of strong cyclonic shear, which in turn produced a cyclonic vortex around the area of lowest surface pressure. To a lesser degree, this shear aided in forming the other cyclonic vortex, near Koror, but a source of positive vorticity from a mid-latitude trough was probably its primary impetus. The cyclonic cell over the Caroline Islands, during its growth into a tropical cyclone, continued to strengthen the Northern Hemisphere NET.

Figure 19 shows that the "cross-equatorial drift" into the Southern Hemisphere was completely cut off. As a result, the Southern Hemisphere NET weakened and skies were almost cloudless over northern Australia and its surrounding waters. Relatively clear skies over western Indonesia allowed the islands to heat and an anticyclone developed over the relatively cool Timor Sea. Outflow from the anticyclone was split, flowing both eastward and westward along the equator. The eastward flow recurved northward into Tropical Depression (T.D.) Nancy, while the westward flow produced mild subsidence over western

Indonesia and further contributed to the suppression of convection. T.D. Nancy intensified and moved northwest toward Truk.

The ESSA 9 satellite composite (Figure 20) indicates intense convection surrounding Nancy and also testifies to strong anticyclonic flow at the cirrus level. The indicated flow to the west of Nancy is not supported by the 250 mb analysis (Figure 21), but is in harmony with the circulation patterns at 300 millibars and at levels above 250 millibars.

Large anticyclones remained over Australia at the 700 and 500 mb levels (Figures 22 and 23). At 700 millibars, the trough which normally extends to 100°E reached only to 135°E and further weakened the Southern Hemisphere NET. The outflow from these anticyclones was divided, flowing westward into Typhoon Judy and eastward into T.D. Nancy.

The divergence pattern (Figure 24) indicates weak divergence to the west of Nancy, but weak convergence over her. The convergence over Nancy is consistent with indicated geopotential height rises over Truk during the 18th (see Figure 9). Negative divergence of  $-1.6 \times 10^{-5} \text{ sec}^{-1}$  over Ponape is questionable since Figure 10 shows geopotential heights to be falling over the island. The 250 mb vorticity analysis shows Nancy to be under an area of zero vorticity with positive values to the west and negative values in all other directions. The KE over

Nancy was about  $20 \text{ m}^2 \text{ sec}^{-2}$ , or one-seventh its value on the 17th.

The surface winds and geopotential height falls at the surface at Truk (see Figure 9) indicate that Nancy passed just to the south of the island at about 18Z on the 18th, when the station exhibited a minimum surface pressure of 1004.7 millibars. During the 18th, 6.17 inches of rain was recorded on Truk and the island experienced absolutely no sunshine. The 12Z 18 February sounding at Truk should be indicative of the vertical structure of T.D. Nancy, but unfortunately, no data was received above 405 millibars. However, from the surface through 450 millibars, temperatures were as much as  $2^\circ\text{C}$ . warmer at 12Z than at 00Z on the 18th. Table 6 indicates that the lower and middle troposphere over Truk was considerably drier at 12Z than at 00Z. The above suggest that the core of Nancy was warmer, but drier, than its surroundings, during the tropical depression stage.

The 00Z 19 February surface analysis (Figure 25) shows the restoration of the "cross-equatorial drift", returning low level convergence to Indonesia. All of Indonesia, except Sumatra, exhibited increased convection. The Southern Hemisphere NET was weak, but visible, from the Solomon Islands to the Gulf of Carpentaria. T.D. Nancy was located near, but southwest of Truk.

The 250 mb analysis (Figure 26) attests to a radical

change in the upper circulation over the Caroline Islands. Southwest winds were observed at Ponape, placing a cyclone between Ponape and Truk. The 300 mb circulation acquired the same feature, but somewhat earlier, suggesting that the cyclonic flow penetrated from lower levels (see Figure 10). Figure 9 indicates that the cyclonic circulation penetrated to 200 millibars.

It is not clear what induced this cyclonic circulation but a possible explanation follows. On the 17th, the 500 mb outflow from the anticyclone over Australia was northward, recurving into westerly flow along the equator in the "equatorial bridge"<sup>4</sup> mode. Near 150°E, this flow divided, curving cyclonically into the Northern and Southern Hemispheres in response to lower pressure. It appears that sometime between 00Z on the 17th and 00Z on the 18th, accelerations occurred which induced the westerly winds to spread from the middle troposphere, up through higher levels, reaching the 250 mb level near the Caroline Islands sometime prior to 00Z on the 19th. The resulting injection of positive vorticity extended the 500 mb cyclonic circulation (see Figure 23) throughout the upper middle troposphere. This further increased the intensity of Nancy and primed her for tropical cyclogenesis. The

---

<sup>4</sup> Described by Johnson and Mörth (1960) as westerly flow between two regions of lower pressure.

residual cyclonic circulation appeared also to have severed the outflow to the mid-latitude westerlies (at 200, 250 and 300 millibars).

The ESSA 9 satellite composite (Figure 27), taken at about 05Z on the 19th, indicates some outflow to the mid-latitude westerlies. The outflow may have been at higher levels, or by 05Z, the 300, 250, and 200 mb flow might have been restored to southeasterly.

The Truk time section (Figure 9) shows that at 00Z on the 19th, geopotential height falls occurred throughout the atmospheric column. Since Nancy was moving away from Truk, the change at Truk indicates larger changes over the tropical depression. Isopleths of  $\theta_e$  show instability in the middle and lower troposphere. The atmospheric column above 700 millibars dried considerably and rain stopped at Truk. This, and the lower level drying at 12Z on the 18th, suggest that a dry tongue existed on the east side of T.D. Nancy.

The 250 mb divergence pattern (Figure 28) shows that Nancy was under a region of nearly zero divergence, with a maximum value of  $3.7 \times 10^{-5} \text{ sec}^{-1}$  some 300 miles to the north of her. It appears that the absence of an outflow channel to the mid-latitude westerlies at the 200, 250 and 300 mb levels prevented the strong divergent flow to the north from effectively removing mass and heat from the environment of Nancy; thus, when southeasterly flow was

reestablished a large gradient of divergence existed between the upper environment of the vortex and the regions north and northeast of it.

Nancy remained under an area of zero vorticity and had positive vorticity to the east, south, and west and negative vorticity to the north and northeast. The KE above the region of Nancy was  $35 \text{ m}^2 \text{ sec}^{-2}$ , nearly twice its value on the 18th.

The surface analysis at 12Z on the 19th (Figure 29) shows that Nancy was approximately 100 km northwest of Truk. The angles of the winds at the 700 and 500 mb levels at Truk suggest that the radius of Nancy decreased with height (see Figures 30 and 31).

With southeasterly flow reinstated at the 250 and 300 mb levels over the Carolines, the stage was set for tropical cyclogenesis (Figure 32). The rapid intensification required to transform Nancy from a tropical depression into a tropical storm occurred near 12Z on the 19th. The rapid changes in the 200, 250 and 300 mb circulation may have been the impetus that triggered her development.

Figure 33 shows that Nancy was under an area of weak convergence ( $-3 \times 10^{-6} \text{ sec}^{-1}$ ), with divergence to the northeast exceeding  $1.9 \times 10^{-5} \text{ sec}^{-1}$ . Nancy continued to remain beneath an area of zero vorticity at the 250 mb level. Except to the west, negative vorticity pre-

dominated, exceeding  $-4.7 \times 10^{-4} \text{ sec}^{-1}$  to the north-northeast where divergence was a maximum. The KE over Nancy was  $55 \text{ m}^2 \text{ sec}^{-2}$  and it appears from changes in the KE field that, by 12Z on the 19th, she was linked to the mid-latitude westerlies at least at the 250 mb level.

Tropical cyclogenesis was occurring during 12Z on the 19th. The large geopotential height falls exhibited throughout the upper troposphere and the lower stratosphere are indicative of much larger geopotential height falls over Nancy, again suggesting that changes over a large region of the upper troposphere are related to intense changes over a small area at the surface.

The isohumes indicate a rapid flux of moisture up through the 230 mb level at Truk, suggesting that, as large or larger fluxes of moisture were occurring in the vicinity of Nancy. Since Nancy was moving away from Truk, we would expect surface pressures at the island to rise, but from 18Z on the 18th to 18Z on the 19th, the surface pressures fell from 1004.7 millibars to 1003.4 millibars. This is a reflection of the very rapid and strong intensification of Nancy (located about 100 km to the northwest).

Could the rapid and deep surge of moisture observed at 12Z on the 19th and the higher than normal sea surface temperatures (SST) combine to facilitate the development of Nancy? Byers (1944) determined that air in the inflow layer of a tropical cyclone is subject to cooling and

drying by decompression as it moves towards lower pressure. That cooling and drying are not observed, moved Riehl (1954) to conclude that both sensible and latent heat are given up by the ocean to the surface air. Malkus and Riehl (1960) indicate that the defect of sea-level pressure ( $p_0$ ) follows the rule--

$$\delta p_0 (\text{mb}) \approx 2.5 \delta \theta_e (^\circ\text{K}) \quad (1)$$

in the tropical range of  $\theta_e$ . Palmén and Newton (1969) state that with "typical saturation deficits at the surface,  $\theta_e$  changes by about  $4.4^\circ\text{K}$  for each  $1^\circ\text{C}$  change of surface temperature"; thus,  $-\delta p_0 (\text{mb}) \approx 11 \delta T_0 (^\circ\text{C})$ . They further conclude that, since the above expressions neglect the contribution of the warmer air within the eye, the sensitivity of the lowest possible pressure to the surface temperatures is even greater. The higher than normal SST would provide a greater than normal  $\theta_e$ , which through (1), would produce a lower surface pressure. The higher  $\theta_e$  would also increase baroclinity and consequently, the production of kinetic energy.

The flux of moisture at 12Z on the 19th reduced the lifting condensation level (LCL) at Truk from 885 millibars at 00Z to 950 millibars at 12Z. The 00Z sounding shows that a parcel of air with the same temperature as the sea surface ( $29^\circ\text{C}$ .), lifted adiabatically from the lowest layers of the atmosphere to the LCL (885 millibars)



and further lifted moist adiabatically to 12 km, would acquire a temperature of  $-59.6^{\circ}\text{C}.$ , or  $6.6^{\circ}\text{C}.$  cooler than the environment at that level. However, the 12Z sounding shows that a parcel undergoing an identical process, with the LCL at 950 millibars, would acquire at 12 km, a temperature of  $-48^{\circ}\text{C}.$ , or  $4.8^{\circ}\text{C}.$  warmer than the environment. Thus, one very important effect of the increase of moisture was to lower the LCL, which resulted in replacing negatively buoyant parcels with positively buoyant ones, a situation compatible with the strong rising motion observed in tropical cyclones. A SST of  $28^{\circ}\text{C}.$  produced a parcel  $3.4^{\circ}\text{C}.$  warmer than the environment at 12 km, while at  $27^{\circ}\text{C}.$  SST rendered the parcel  $0.7^{\circ}\text{C}.$  cooler than the environment at 12 km (both cases using a LCL of 950 millibars). Figure 18 indicates that in a normal February the SST gradient in the region where Nancy developed, is directed from north to south across the equator. Therefore, the rareness of "off-season typhoons" may, in part, result from the rareness of a SST maximum north of the equator.

From 00Z to 12Z on the 19th, isentropic surfaces in the upper troposphere and lower stratosphere over Truk were elevated and the tropopause rose 35 millibars. These elevations indicate an upward flux of heat. From 00Z on the 18th to 00Z on the 19th, temperatures at the 100 mb level fell  $2^{\circ}\text{C}.$  and on the 19th from 00Z to 12Z they fell an additional  $2^{\circ}\text{C}.$  at this level and also at the 250 mb

level. This suggests considerable heat flux divergence in the upper troposphere during this period. Also between 00Z and 12Z on the 19th, cooling occurred above 400 millibars, while warming occurred below.

The Fleet Weather Central/Joint Typhoon Warning Center at Guam declared Nancy a tropical storm at 23Z on the 19th, but at this time she already possessed 60 knot winds at the 700 mb level and 55 knot winds at the surface. Thus, sometime between 12Z and 23Z on the 19th, T.S. Nancy was born.

The 00Z 20 February surface analysis (Figure 34) shows the continued reestablishment of the Southern Hemisphere NET, as evidenced by the convective activity just north of Australia (Figure 35). T.S. Nancy moved westward, paralleling the upper tropospheric subtropical ridge. The 250 mb analysis (Figure 36) suggests a large outflow channel to the northeast of Nancy and both the 20 February and 21 February ESSA 9 satellite mosaics indicate upper tropospheric outflow to the mid-latitude westerlies (Figures 35 and 37).

Figure 38 shows that Nancy was surrounded by divergence at the 250 mb level, which exceeded  $3.6 \times 10^{-5} \text{ sec}^{-1}$  from the north through the east. The vorticity pattern shows Nancy embedded in positive vorticity (she possessed a cyclonic circulation up through 250 millibars),

with positive vorticity to the west and negative vorticity in the remaining areas. The 250 mb KE analysis indicates strong outflow to the northeast from Nancy and weak outflow to the south. Figure 9 indicates a considerable drying throughout the atmospheric column over Truk; strong subsidence was responsible.

Tropical storm Nancy continued westward at 10 to 12 knots and achieved typhoon intensity during mid-day of the 22nd about 100 miles northwest of Woleai Atoll. On the morning of the 23rd, she approached Yap Island where she began to further intensify. Some 330 miles east of Leyte, she approached the southwestern periphery of the subtropical ridge and began to recurve to the north. About 90 miles east of Samar she reached peak intensity of 120 knots which was maintained until after she struck Catanuanes Island, about 100 miles to the northwest. Nancy slowly weakened as she approached the mid-latitude westerlies and became a tropical storm on the 26th. She became extratropical on the 27th, her dissipation resulting from a combination of strong shear in the westerlies and the incursion of cold air at the surface.

#### 2.4. Summary and Conclusions

At the beginning of the study, the question was posed: how do "off-season typhoons" differ from other typhoons in their formation and development? Several requirements for the formation of tropical cyclones were listed. How did

the "off-season typhoon", Nancy, conform to the requirements? She: (1) formed over a large ocean area with high sea surface temperatures (28-29°C.); (2) developed into a tropical storm in an area where vertical shear was small above her core; (3) developed poleward of 8°N latitude; (4) developed from a pre-existing, low level disturbance; and, (5) possessed upper tropospheric outflow above the region of development.

A more extensive look at these requirements reveals features that were particularly important in the formation and development of Nancy.

Sea surface temperatures were 1° to 2°C. above normal and exhibited a maximum about 4° latitude north of the equator. The sea surface temperature maximum north of the equator (1) provided a region where a thermally induced near-equatorial trough could form and (2) thermally anchored the strong Northern Hemisphere near-equatorial trough that was associated with the formation of Nancy. This maximum sea surface temperature contributed to the development of Nancy in the following ways: (1) It provided a source of moist air, which when lifted from the lowest levels and expanded pseudo-adiabatically, remained considerably warmer than the environment, thus enhancing upward motion in the manner observed in mature tropical cyclones. (2) It provided a greater than normal potential for the flux of both sensible and latent heat to the

central regions of the storm, increasing the gradient of  $\theta_e$  and ultimately the generation of kinetic energy.

The initial low pressure area formed where vertical shear exceeded 25 knots between the 850 and the 200 mb levels. As convection increased, upper level wind speeds decreased, such that prior to development of Nancy into a tropical storm, her core was beneath a vertical shear less than 10 knots between the 850 and the 200 mb levels.

The initial low pressure area of the disturbance developed south of  $5^\circ\text{N}$  and was visible as a relatively clear area surrounded by intense convection; consequently, the distribution of condensed water in the troposphere surrounding the low pressure area intensified the pressure gradient which further increased development of the low pressure area. Further intensification into a tropical depression occurred poleward of  $6^\circ\text{N}$  and intensification into a tropical storm transpired poleward of  $8^\circ\text{N}$ .

We earlier asserted that a considerable alteration in the general low level circulation must occur if the initial tropical vortex were to develop in a shear zone. In the case of Nancy, the initial vortex did form in such a shear zone. No easterly waves or equatorial waves were observed during her formation and development. It seems that one requirement for the formation of "off-season typhoons" is one of westerly winds north of the equator. That tropical westerlies are normally confined to the Southern Hemisphere

during the Northern Hemisphere winter, accounts, at least in part, for the rareness of "off-season typhoons."

The upper outflow over Nancy during her development into and her existence as a tropical storm, was the result of strong upper tropospheric divergence associated with the penetration into the tropics of an upper level, mid-latitude trough. From 12Z on the 19th to 00Z on the 20th, the 250 mb divergence above the storm increased from  $-5 \times 10^{-6} \text{ sec}^{-1}$  to  $2 \times 10^{-5} \text{ sec}^{-1}$ . The change could have occurred throughout the entire 12 hour period, or over a much smaller span of time. This suggests that perhaps the absolute value of the divergence is not as important in the development of tropical cyclones as the speed at which it occurs. The rapid export of mass could account for large surface pressure falls which occur so rapidly that low level convergence cannot compensate. Burroughs (1974) indicates that the divergence of heat flux is closely related to the divergence of mass. A rapid flux of heat away from the upper environment of the disturbance, by destabilizing the tropical troposphere, would increase upward motion and convection. This could in turn account for "an in-spiraling of air, massive rising in the central core, and development, through subsidence, of a warm eye"<sup>5</sup>, all before low level convergence could compensate for the

---

<sup>5</sup>C. S. Ramage (1971).

effects of the rapid, upper tropospheric divergence.

Since during the Northern Hemisphere winter, the Northern Hemisphere upper tropospheric ridge is located near  $12^{\circ}\text{N}$  latitude, we earlier hypothesized that cross-equatorial interactions might play an important part in the formation and development of "off-season typhoons." The role of the more apparent of the interactions in the formation and development of Typhoon Nancy are as follows: (1) Large, upper tropospheric, southeasterly, local increases in wind speed which occurred over a wide area of the tropical western Pacific were followed (12-24 hours later) by large, lower tropospheric, northwesterly, local increases in wind speed, just south of the equator, which occurred over a relatively small area. These strong, lower level winds spread the realm of westerlies from south of the equator to north of the equator, resulting in the formation of a Northern Hemisphere near-equatorial trough. Shear between these westerlies and the northeasterlies over the Caroline Islands produced the cyclonic vortex which later became Typhoon Nancy. (2) Middle tropospheric flow from an anticyclone over Australia, provided a source of cyclonic vorticity which extended the cyclonic vortex (which later became Nancy), from the 500 mb level, up through the upper middle troposphere, further intensifying the vortex. As it crossed the equator, the flow from the anticyclone spread up through the 200 mb level and produced

a cyclonic circulation between Truk and Ponape; consequently, outflow to the mid-latitude westerlies at the 200, 250 and 300 mb levels over the intensifying vortex was severed, resulting in weak convergence over the vortex and strong divergence to its northeast. When outflow to the mid-latitude westerlies was reinstated at these levels, the resulting large gradient of divergence between the upper troposphere over the vortex and the regions to the north and northeast, may have triggered the development of the tropical storm.

Finally, in a wider, speculative context we may ask: was Nancy a fluke or was she the combined result of a Southern Hemisphere response to curtail tropical cyclone development, by weakening the Southern Hemisphere near-equatorial trough, and a Northern Hemisphere demand for energy, energy that is usually obtained from intense convection over Indonesia.



Table 1. February 1970 mean 200 mb winds and February long term mean 200 mb winds at Giles (25°02'S, 128°18'E), Alice Springs (23°48'S, 133°53'E), Cloncurry (20°40'S, 140°30'E), and Noumea (22°16'S, 166°27'E). Directions are in degrees (°) and speeds are in knots (k).

	Giles	Alice Springs	Cloncurry	Noumea
February 1970	244° 16k	230° 22k	260° 22k	275° 47k
February mean	257° 32k	261° 26k	273° 16k	291° 32k

Table 2. Gradient level winds from 10-17 February 1970 and the February long term mean gradient level winds (LTM) for Port Moresby (09°26'S, 147°13'E), Lae (06°44'S, 147°00'E), Manus Island [(Momote) 02°04'S, 147°26'E], and Songkhla (07°11'S, 100°37'E). Directions are in degrees (°) and speeds are in knots (k). Data is from 00Z observations. Dashed lines indicate data missing or not available.

GRADIENT LEVEL WINDS

Date	Port Moresby	Lae	Manus Island	Songkhla
10	330° 35k	-----	320° 30k	090° 28k
11	320° 25k	300° 25k	320° 25k	075° 34k
12	300° 50k	280° 50k	300° 20k	065° 26k
13	320° 35k	290° 50k	020° 15k	140° 10k
14	310° 15k	310° 20k	330° 20k	120° 18k
15	310° 20k	-----	-----	085° 20k
16	290° 10k	300° 25k	310° 40k	070° 36k
17	330° 20k	270° 15k	300° 50k	075° 36k
LTM	310° 12k	-----	-----	084° 14k

Table 3. 200 mb winds from 10-17 February 1970 and the February long term mean 200 mb winds (LTM) for Koror (07°20'N, 134°29'E), Truk (07°28'N, 151°51'E), and Ponape (06°58'N, 158°13'E). Directions are in degrees (°) and speeds are in knots (k). Data is from 00Z observations.

200 MB WINDS

Date	Koror	Truk	Ponape
10	130° 34k	133° 26k	145° 42k
11	139° 50k	117° 44k	132° 56k
12	146° 40k	118° 44k	126° 46k
13	145° 22k	120° 44k	128° 42k
14	122° 22k	124° 46k	142° 40k
15	095° 24k	126° 30k	125° 20k
16	130° 26k	122° 48k	144° 58k
17	134° 42k	141° 32k	130° 30k
LTM	119° 24k	122° 16k	117° 17k

Table 4. Surface pressure differences from 10-18 February 1970 and the February long term mean surface pressure differences (LTM) between Hong Kong-Singapore, Hong Kong-Djakarta, Djakarta-Honiara, and Djakarta-Manus Island. Surface pressure differences are in millibars. Data is from 00Z observations. Dashed lines indicate data missing or not available. [Hong Kong (22°18'N, 114°10'E), Singapore (01°21'N, 103°54'E), Djakarta (06°11'S, 106°51'E), Honiara (09°52'S, 159°58'E), Manus Island (Momote) (02°04'S, 147°26'E)].

Date	HK-Sing	HK-Djak	Djak-Hon	Djak-Man
10	11.5	11.7	7.6	5.7
11	12.3	12.3	6.8	5.0
12	10.0	9.8	9.7	5.7
13	8.5	9.1	---	4.8
14	8.3	9.5	4.4	2.9
15	7.2	7.5	5.6	2.3
16	11.6	11.3	4.0	1.6
17	10.4	9.8	3.0	---
18	6.5	7.9	0.1	0.2
LTM	8.2	8.8	2.8	---

Table 5. Five day mean geopotential heights for 6-10 and 11-15 February 1970, February 1970 mean geopotential heights, and February long term geopotential heights at the 700 and 500 mb levels at Alice Springs (23°48'S, 133°53'E), Darwin (12°26'S, 130°52'E), and Cloncurry (20°40'S, 140°30'E). Geopotential heights are in meters. Data is from 00Z observations.

Level	Period	Alice Springs	Darwin	Cloncurry
700 MB	06-10	3166	3129	3132
	11-15	3191	3147	3154
	Feb 1970	3171	3144	3147
	Feb mean	3157	3124	3127
500 MB	06-10	5886	5838	5858
	11-15	5906	5858	5868
	Feb 1970	5882	5860	5861
	Feb mean	5882	5844	5842

Table 6. Dew point depressions for a "normal" tropical sounding at Grand Bahama Island in the Caribbean region (GBI) (from Bhumralkar, 1974) and for Truk Island (07°28'N, 151°51'E) at 00Z and 12Z on 16, 18, and 19 February 1970. Dew point depressions are in degrees Centigrade, to the nearest one-half degree.

Level (mb)	(GBI)	16-00Z	16-12Z	18-00Z	18-12Z	19-00Z	19-12Z
300	10.0	13.0	1.0			14.0	6.0
400	12.0	12.5	0.0			13.0	10.0
500	13.5	10.0	0.0	2.5	4.0	7.0	3.0
600	17.0	19.5	16.0	0.5	7.0	10.0	4.5
700	11.0	19.0	12.5	1.0	11.5	10.5	6.5
850	5.5	5.5	4.0	1.0	10.5	6.0	5.5
1000	7.0	5.5	3.0	1.0	2.0	3.0	4.0

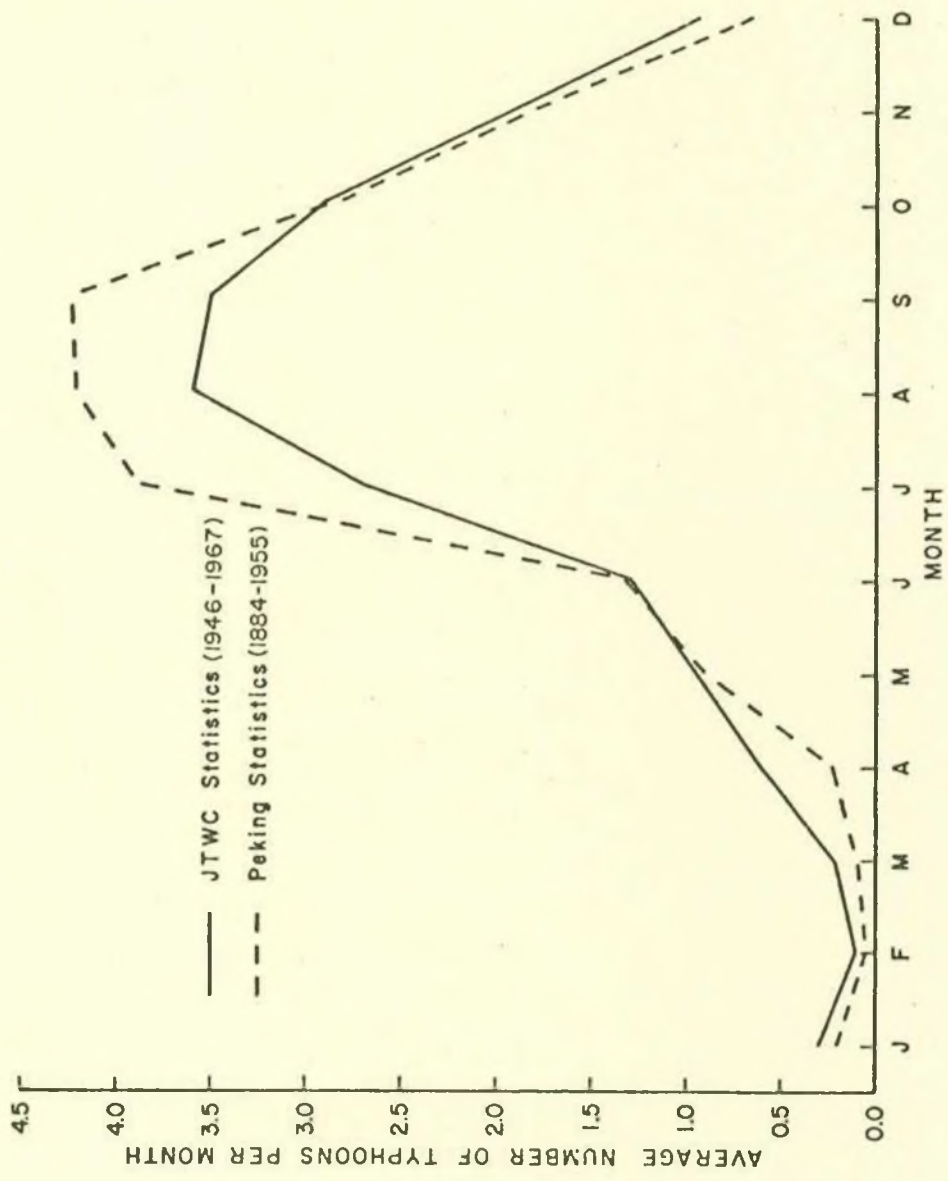


Figure 1. Monthly variation in the average number of typhoons in the western North Pacific (from Gray 1970).

Figure 2. General analysis area for the study.



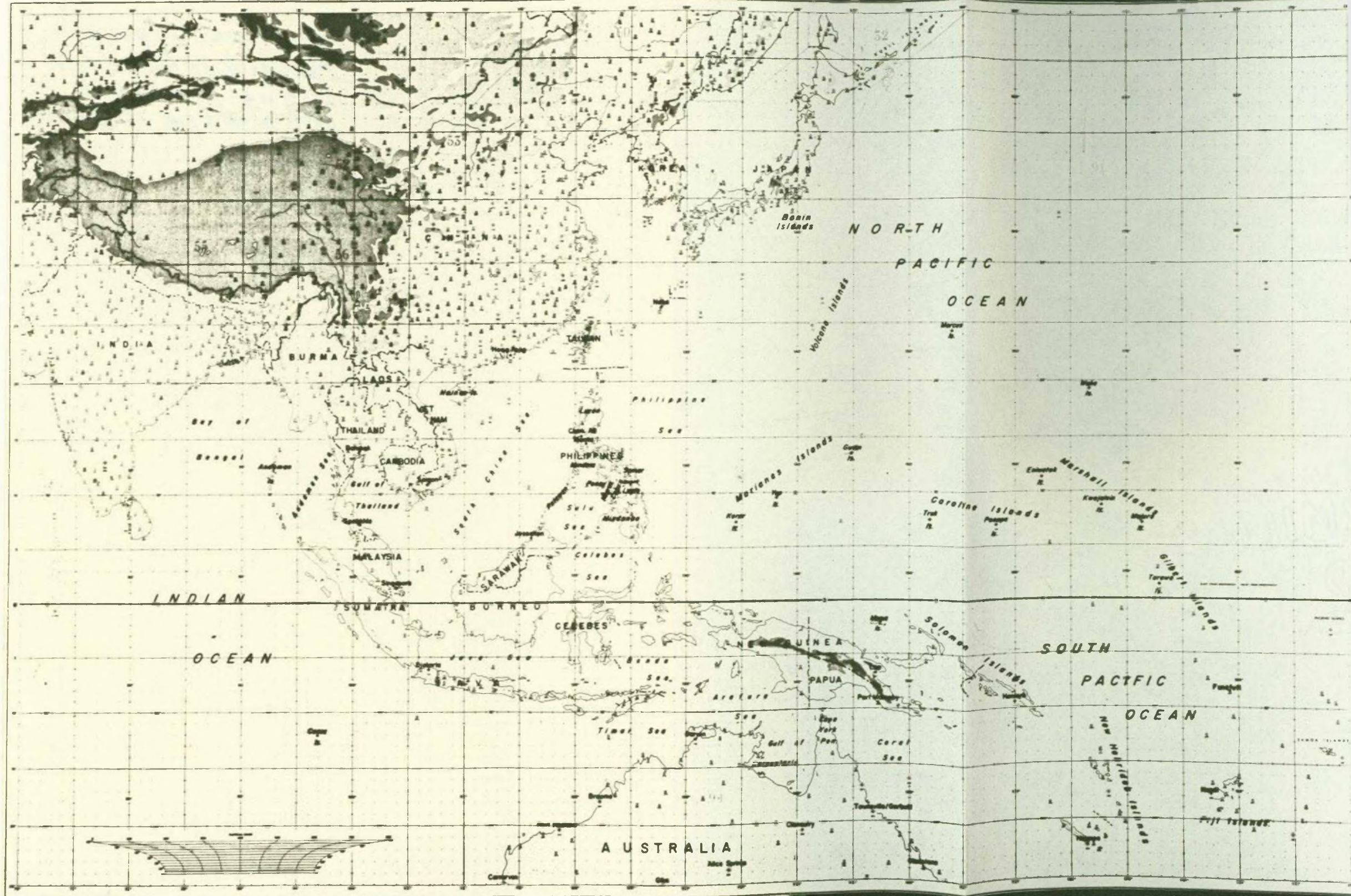


Figure 3. Departures of the mean February 1970 cloudiness from Sadler's February 6 year mean (octas). Hatched areas are above normal, unhatched areas are below normal, upper numbers are departures in octas and lower numbers indicate the sample size in days.

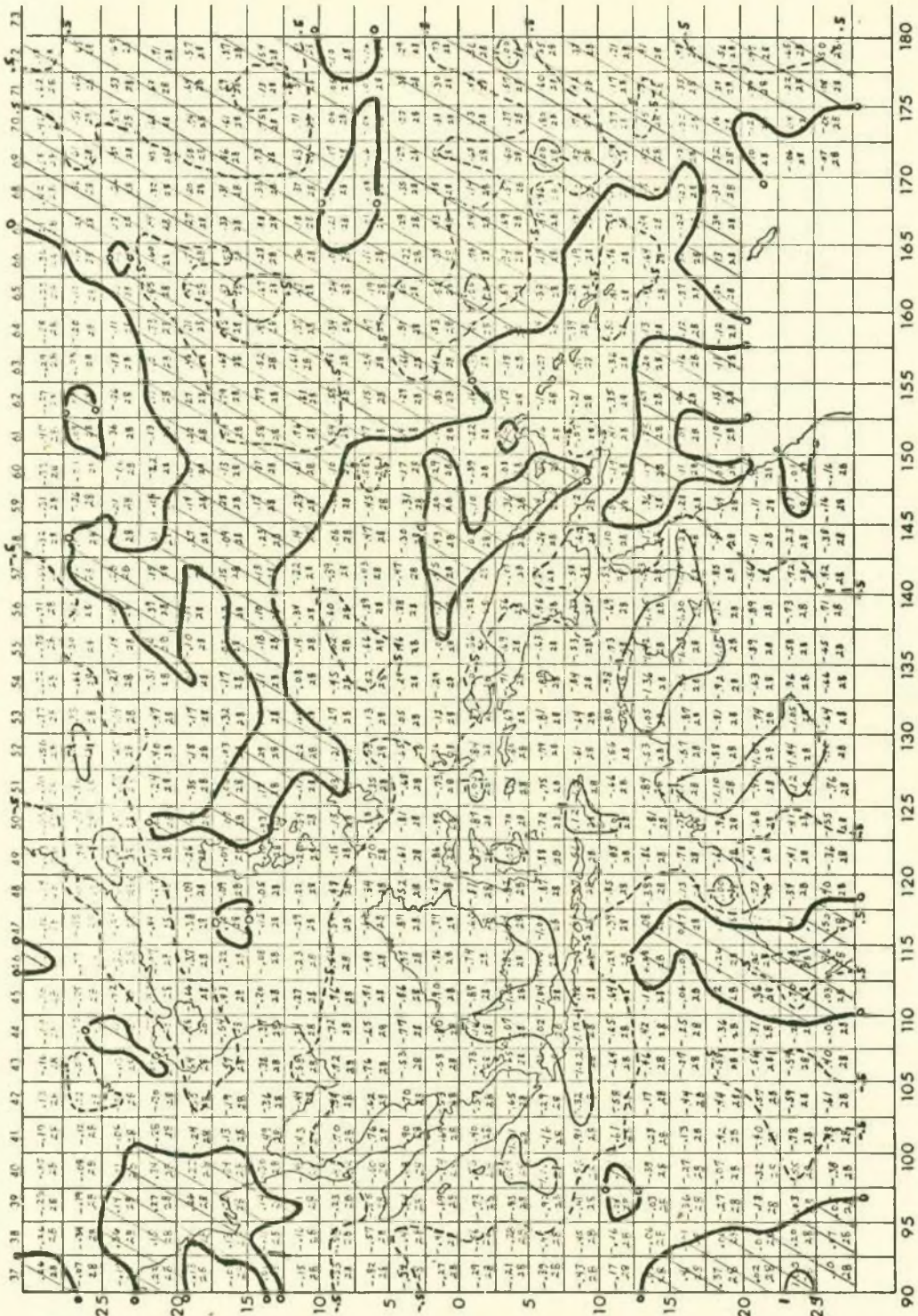
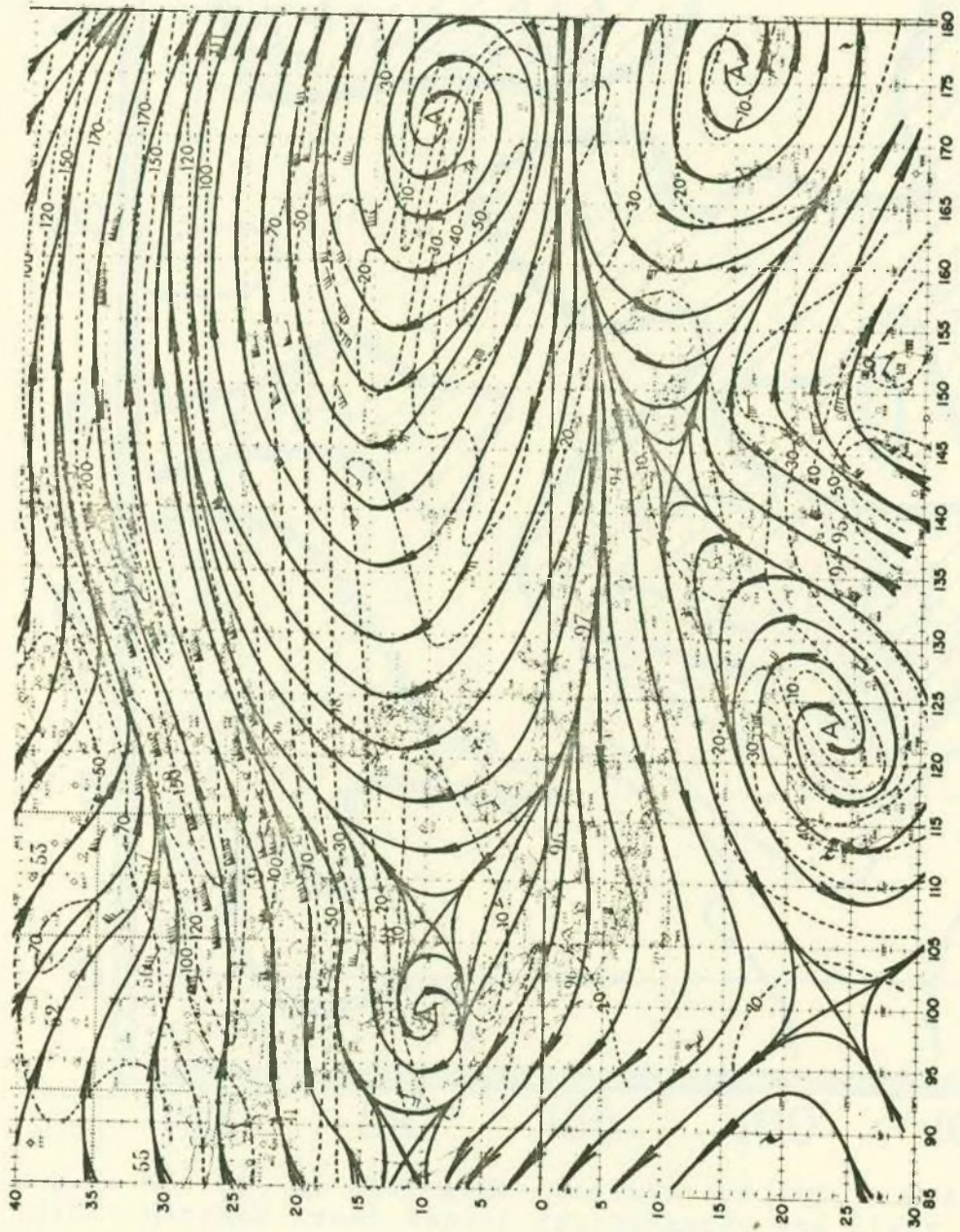


Figure 4. 250 mb streamline and isotach analysis for 00Z 16 February 1970. Streamlines are full and isotachs are dashed (knots). Flags on wind barbs are 50 knots for triangles, 10 knots for full flags and 5 knots for half flags.



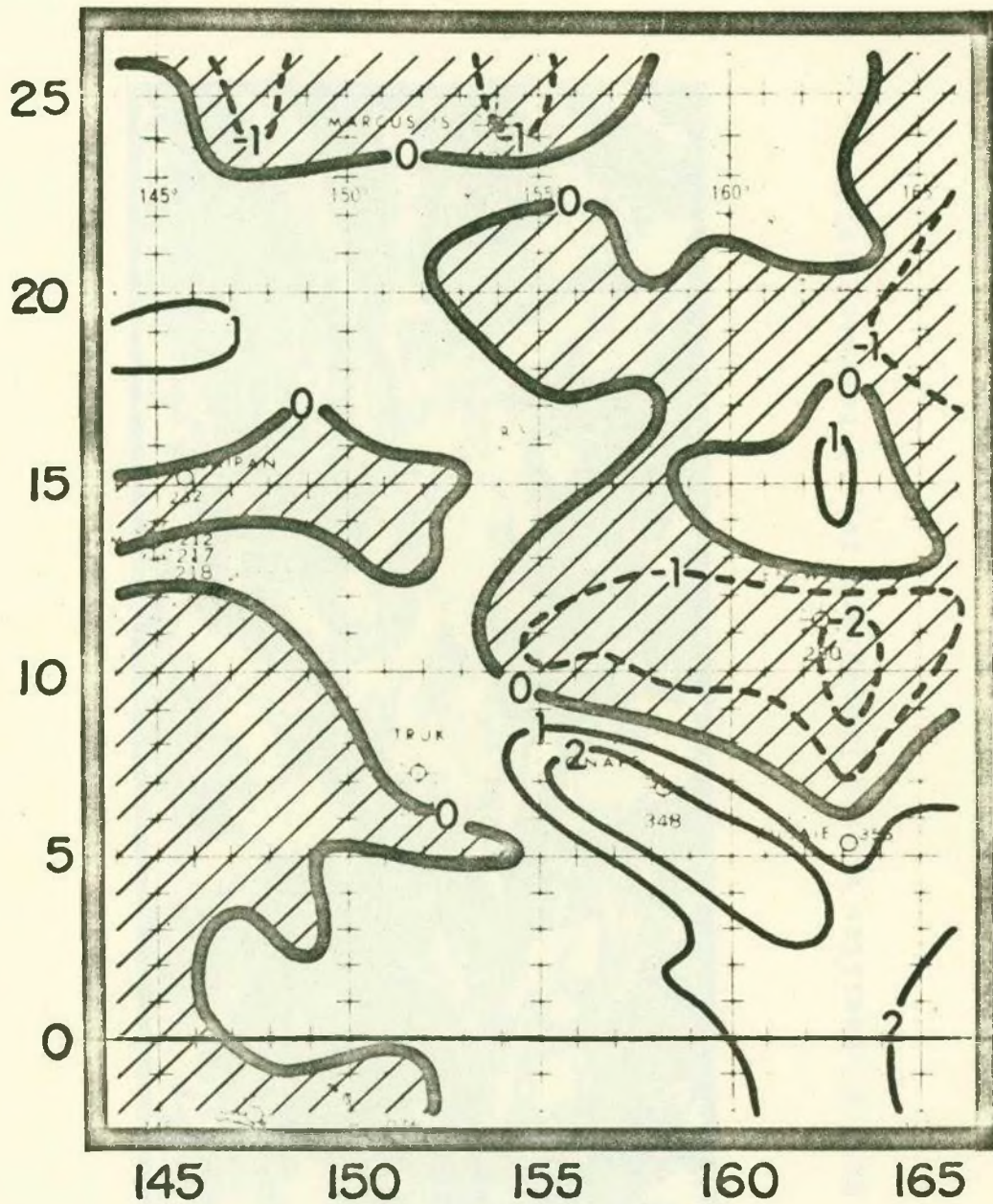


Figure 5. 250 mb divergence pattern for 00Z 16 February 1970. Hatched areas depict convergence, and clear areas depict divergence.

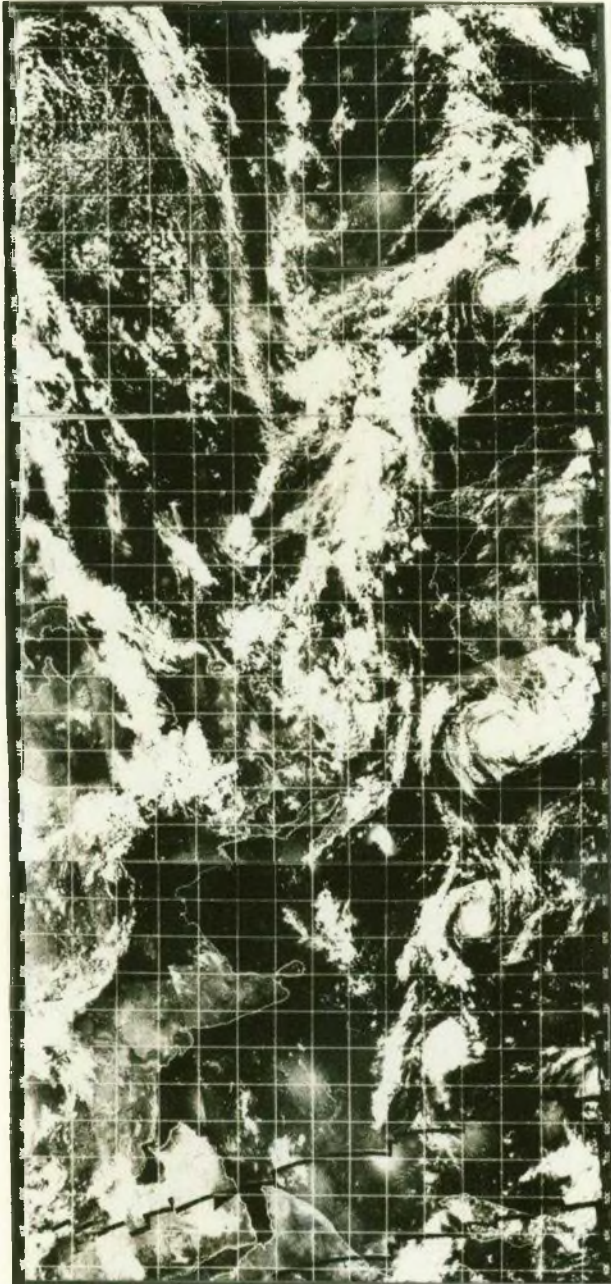


Figure 6. ESSA 9 satellite mosaic photograph for 15 February 1970.

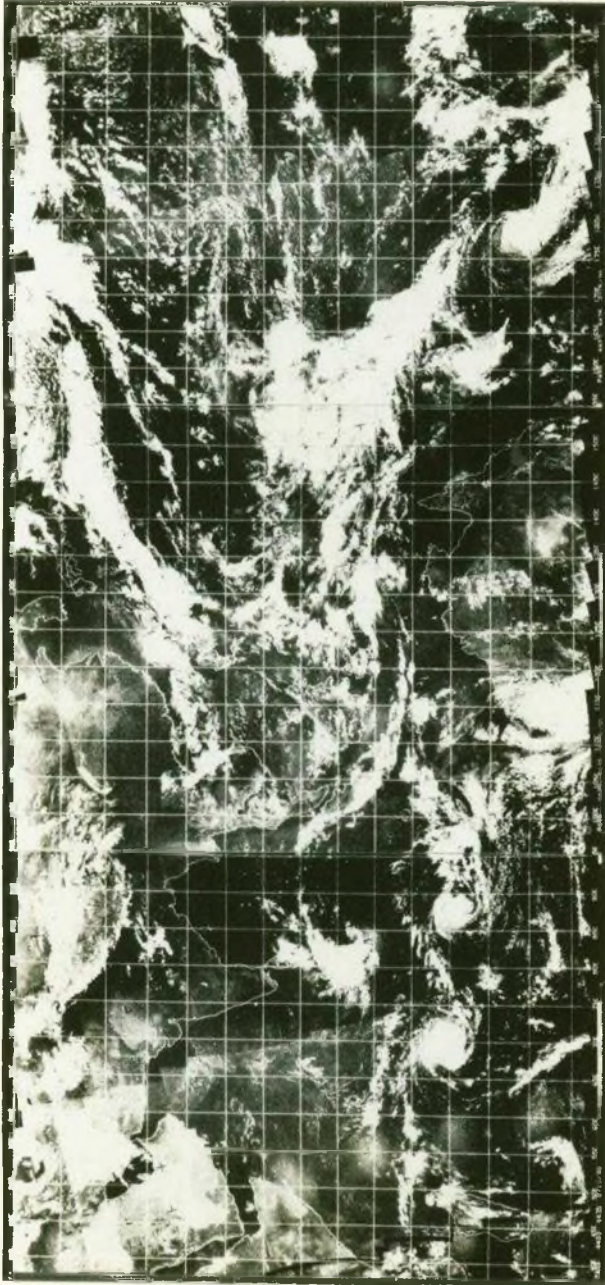


Figure 7. ESSA 9 satellite mosaic photograph for 16 February 1970.



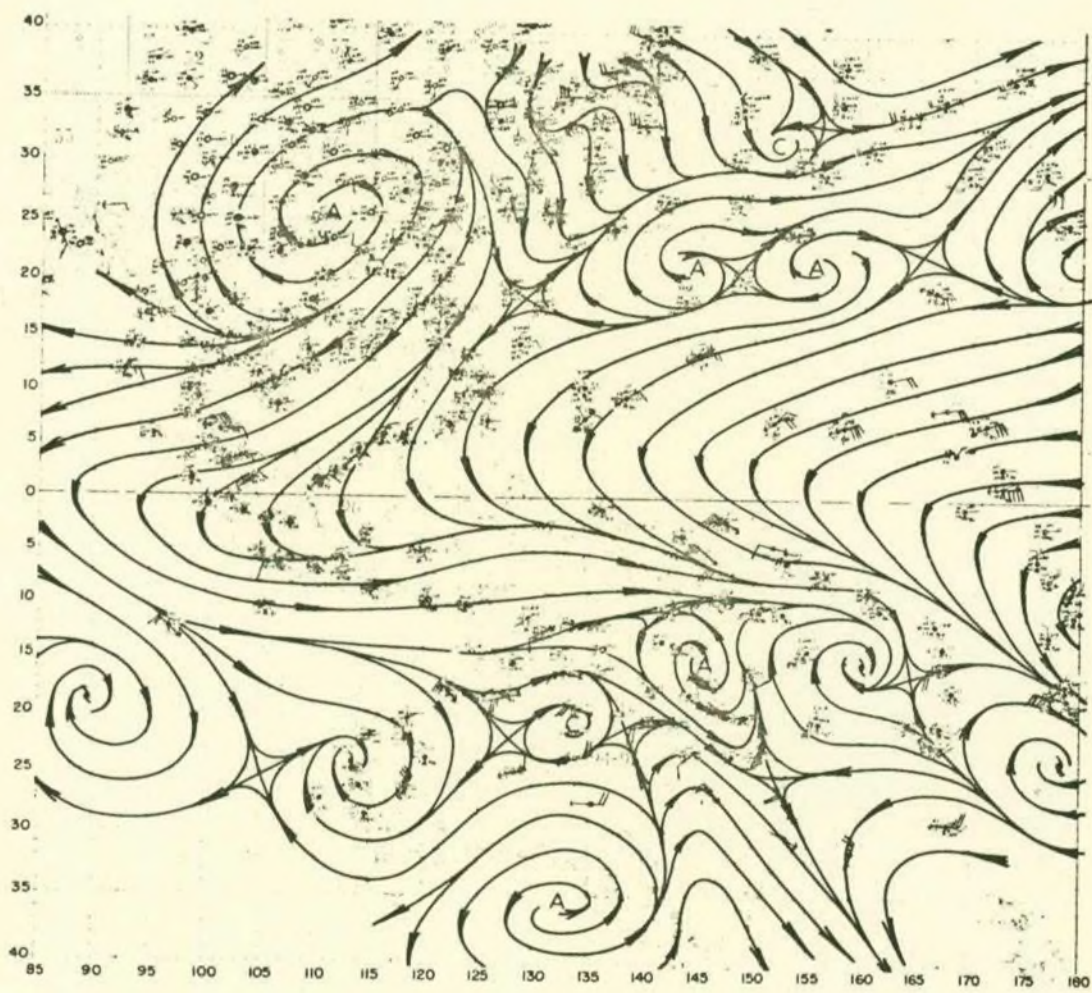


Figure 8. Surface and gradient level streamline analysis for 00Z 16 February 1970. Winds are in knots.

Figure 9. Time cross-section for Truk ( $07^{\circ}28'N$ ,  $151^{\circ}51'E$ ) from 16-20 February 1970. Positive geopotential height differences are shown thick and full (meters), negative geopotential heights are shown thick and dashed (meters),  $\theta_e$  is shown thin and full ( $^{\circ}K$ ), isohumes are shown thin and dashed (percent), the tropopause is shown dotted, and wind speeds are indicated by the flags on the wind barbs (knots). Triangular flags are 50 knots, full flags are 10 knots, half flags are 5 knots and no flags are less than 3 knots. Three hourly observations begin in the lower left corner with 18Z 15 February 1970.

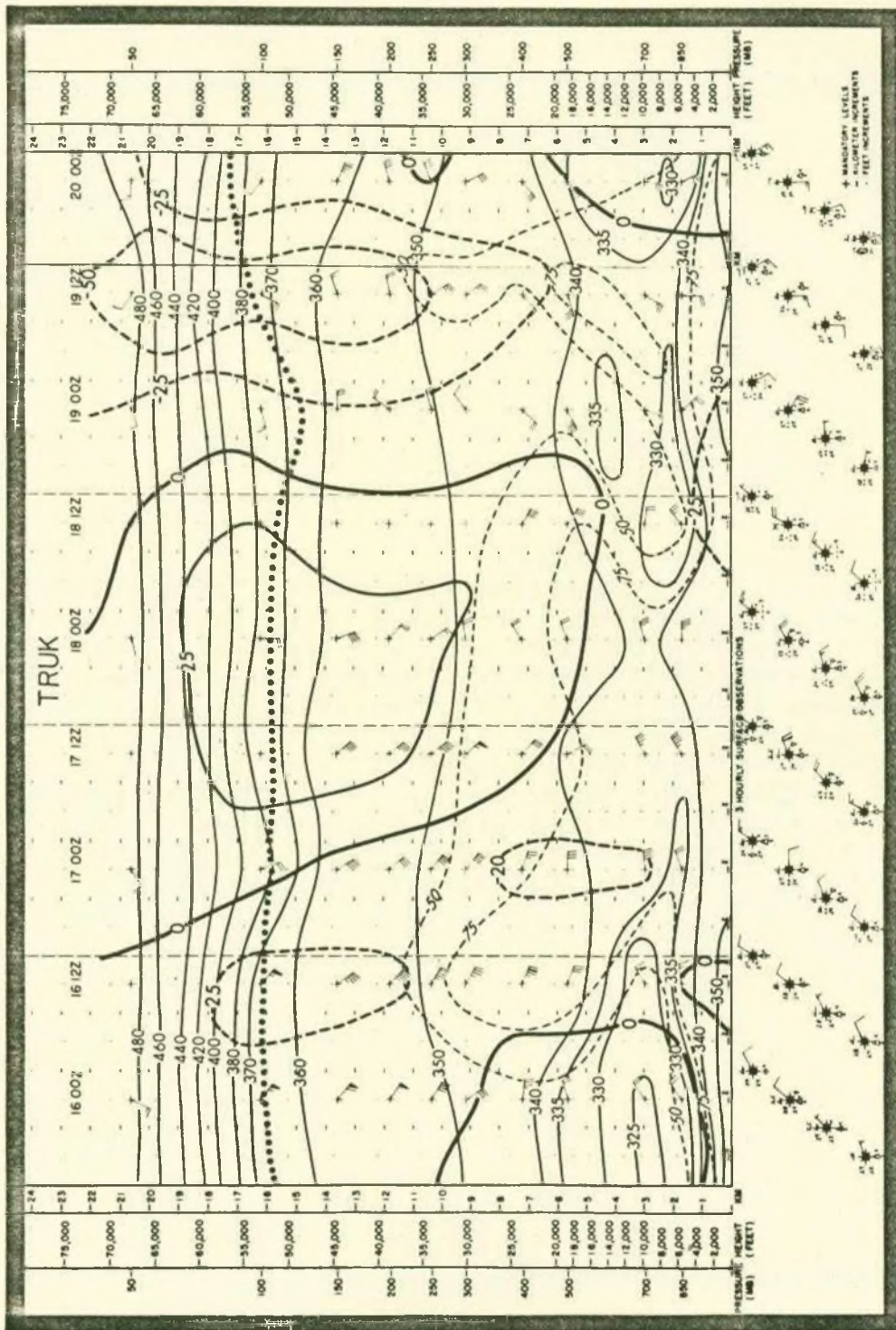
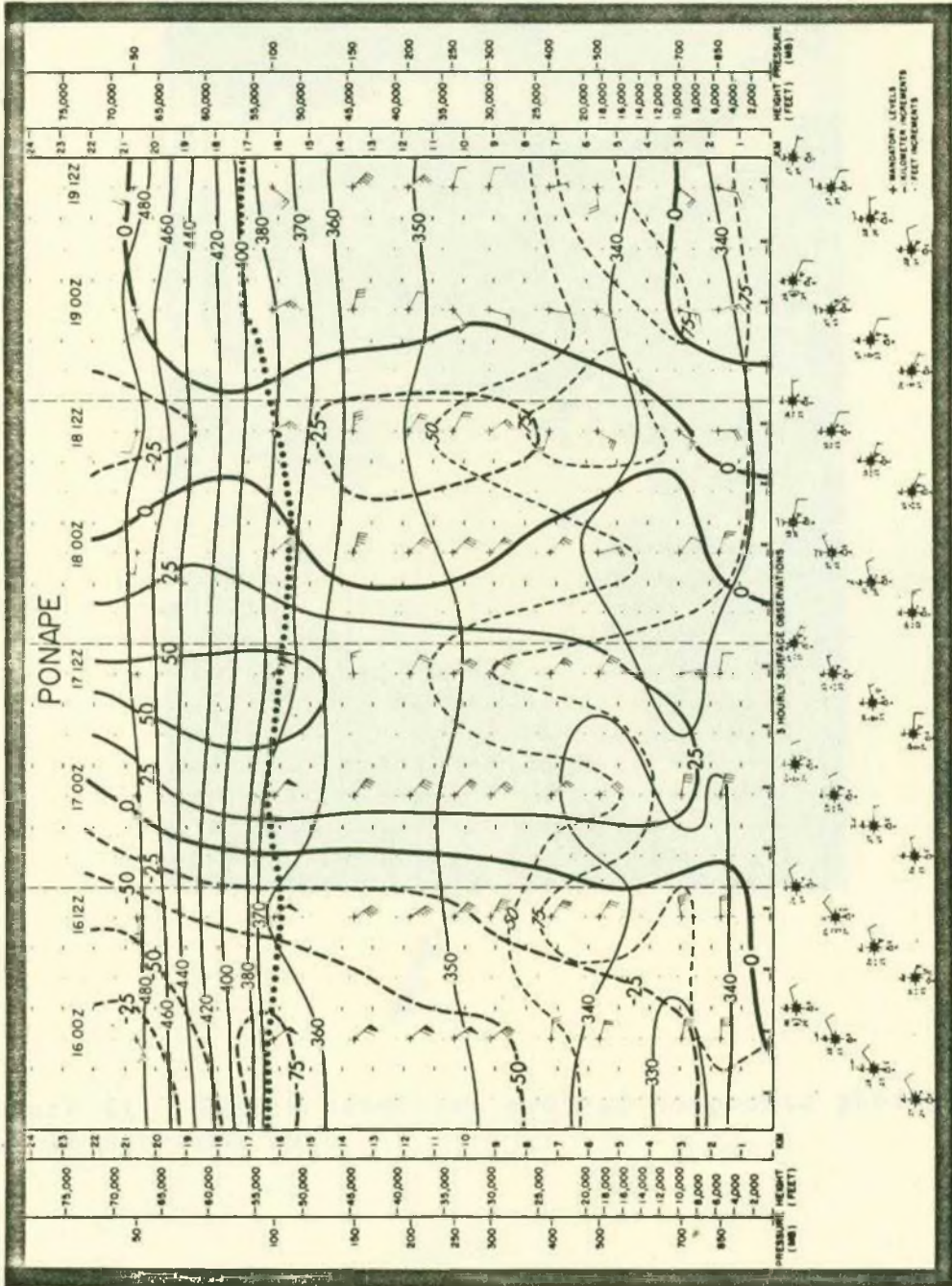


Figure 10. Time-cross section for Ponape ( $06^{\circ}58'N$ ,  $158^{\circ}13'E$ ) from 16-19 February 1970. Positive geopotential height differences are shown thick and full (meters), negative geopotential height differences are shown thick and dashed (meters),  $\theta_e$  is shown thin and full ( $^{\circ}K$ ), isohumes are shown thin and dashed (percent), the tropopause is shown dotted, and wind speeds are indicated by the flags on the wind barbs (knots). Triangular flags are 50 knots, full flags are 10 knots, and half flags are 5 knots. Three hourly observations begin in the lower left corner with 18Z 15 February 1970. (12 hourly fluctuations in the isohumes suggests a poorly ventilated rawinsonde instrument.)



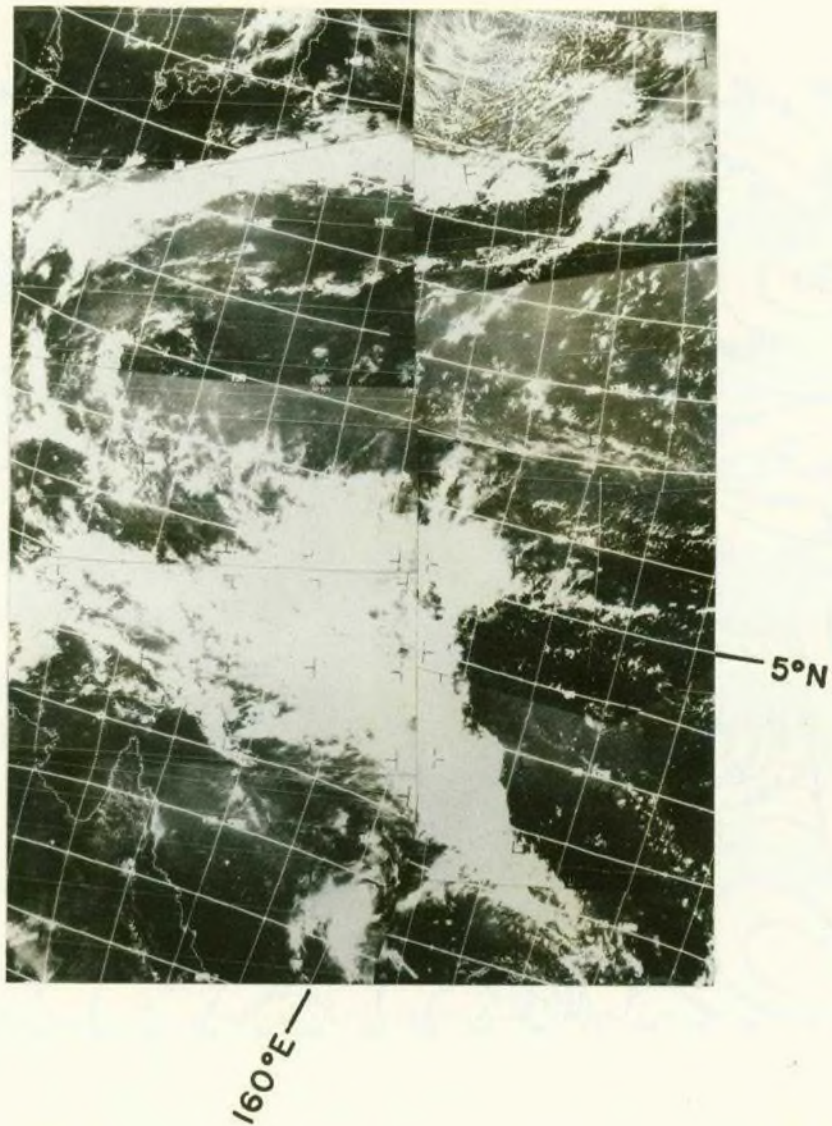


Figure 11. ESSA 9 satellite orbital composite photograph for 16 February 1970.

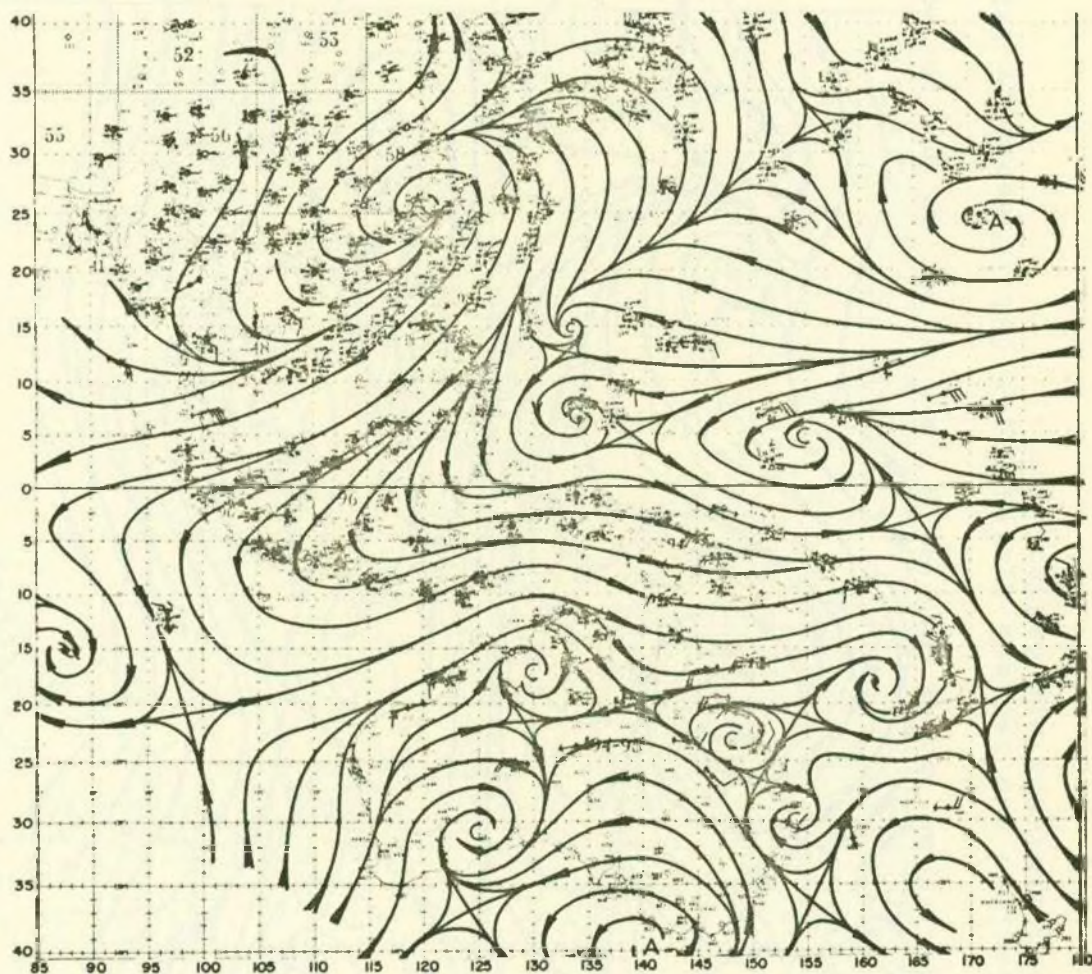


Figure 12. Surface and gradient level streamline analysis for 00Z 17 February 1970. Winds are in knots.

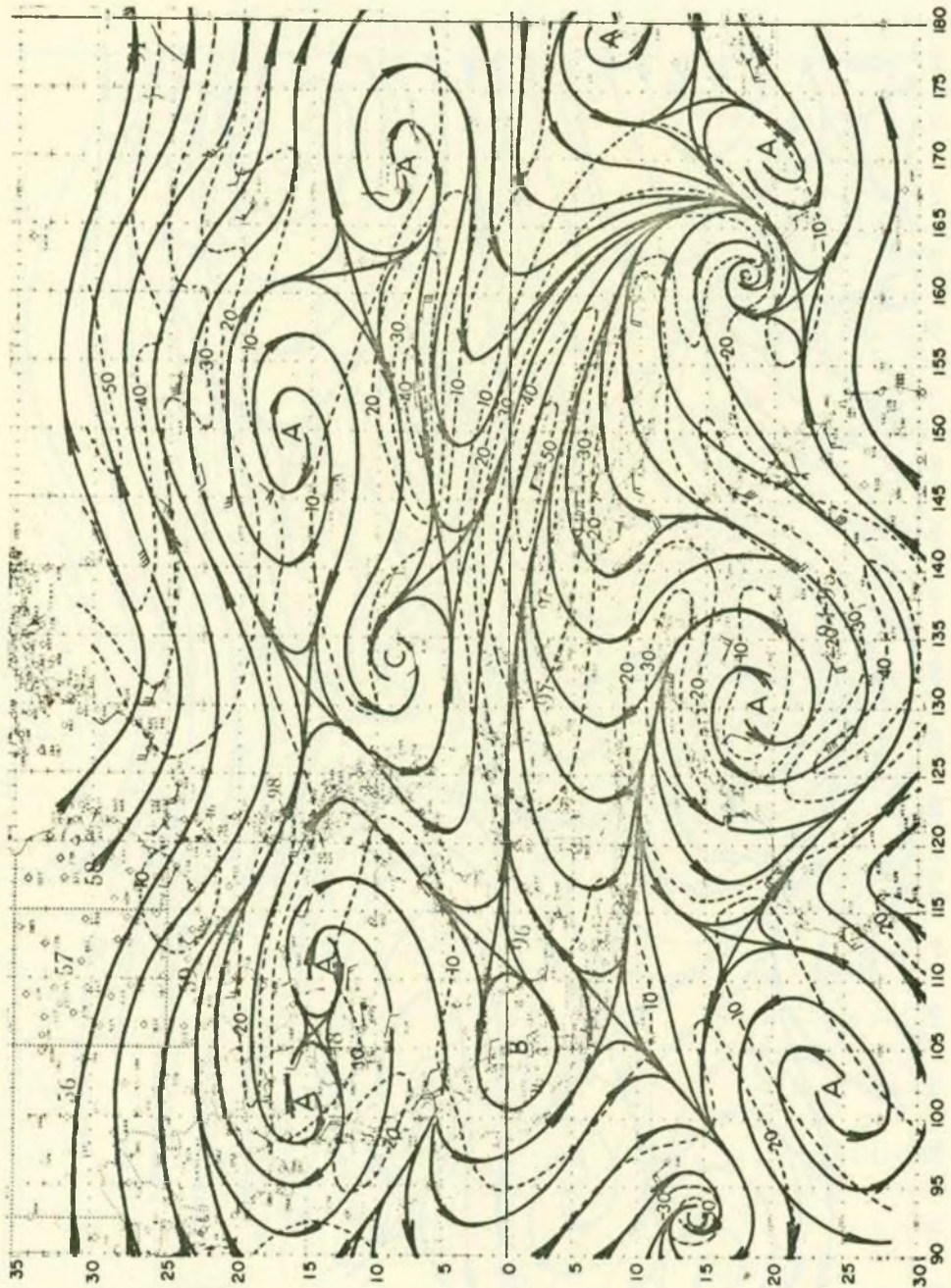


Figure 13. 700 mb streamline and isotach analysis for 00Z 17 February 1970. Streamlines are full, and isotachs are dashed (knots).



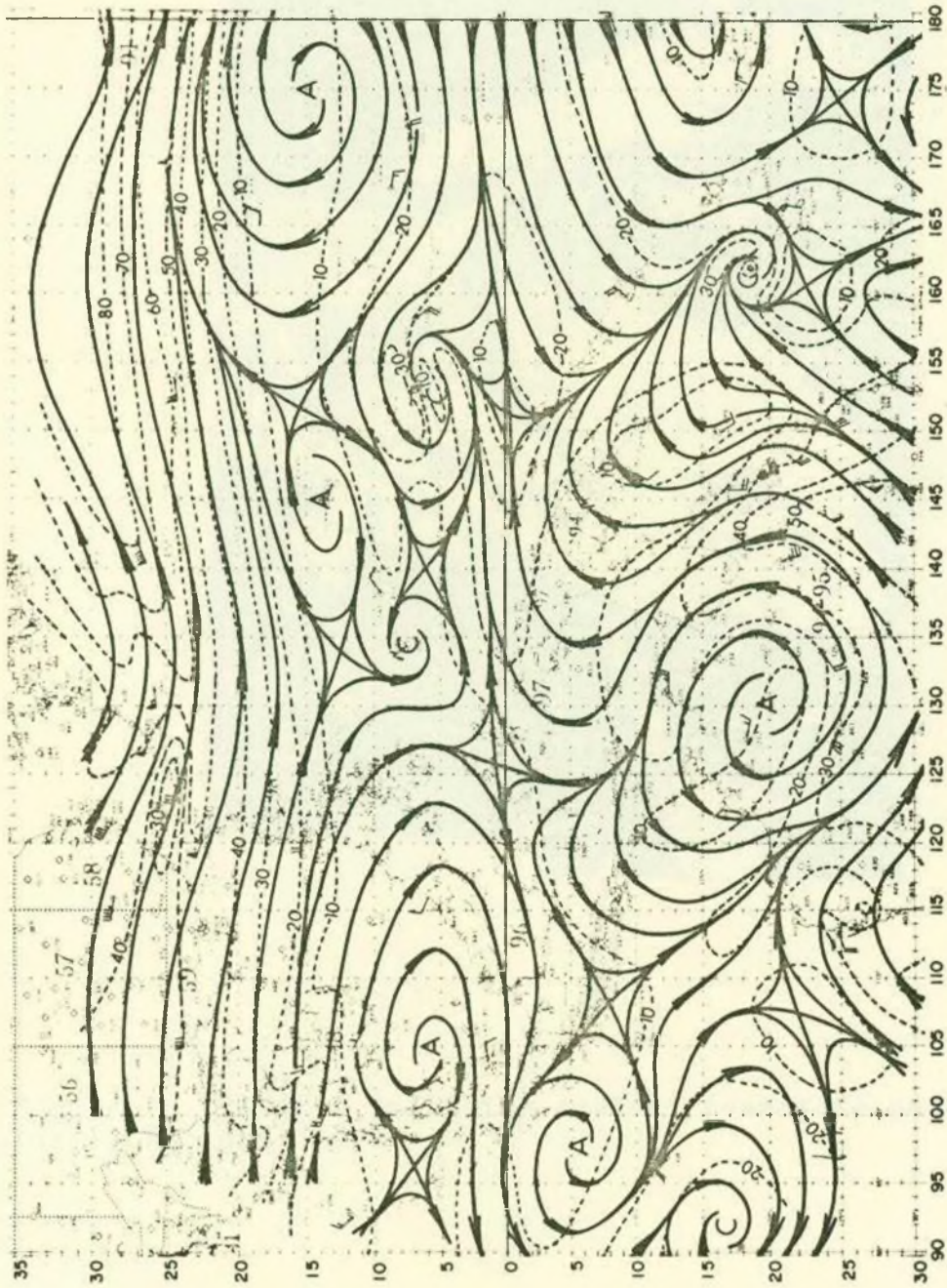


Figure 14. 500 mb streamline and isotach analysis for 00Z 17 February 1970. Streamlines are full, and isotachs are dashed (knots).



Figure 15. ESSA 9 satellite orbital composite photograph for 17 February 1970.

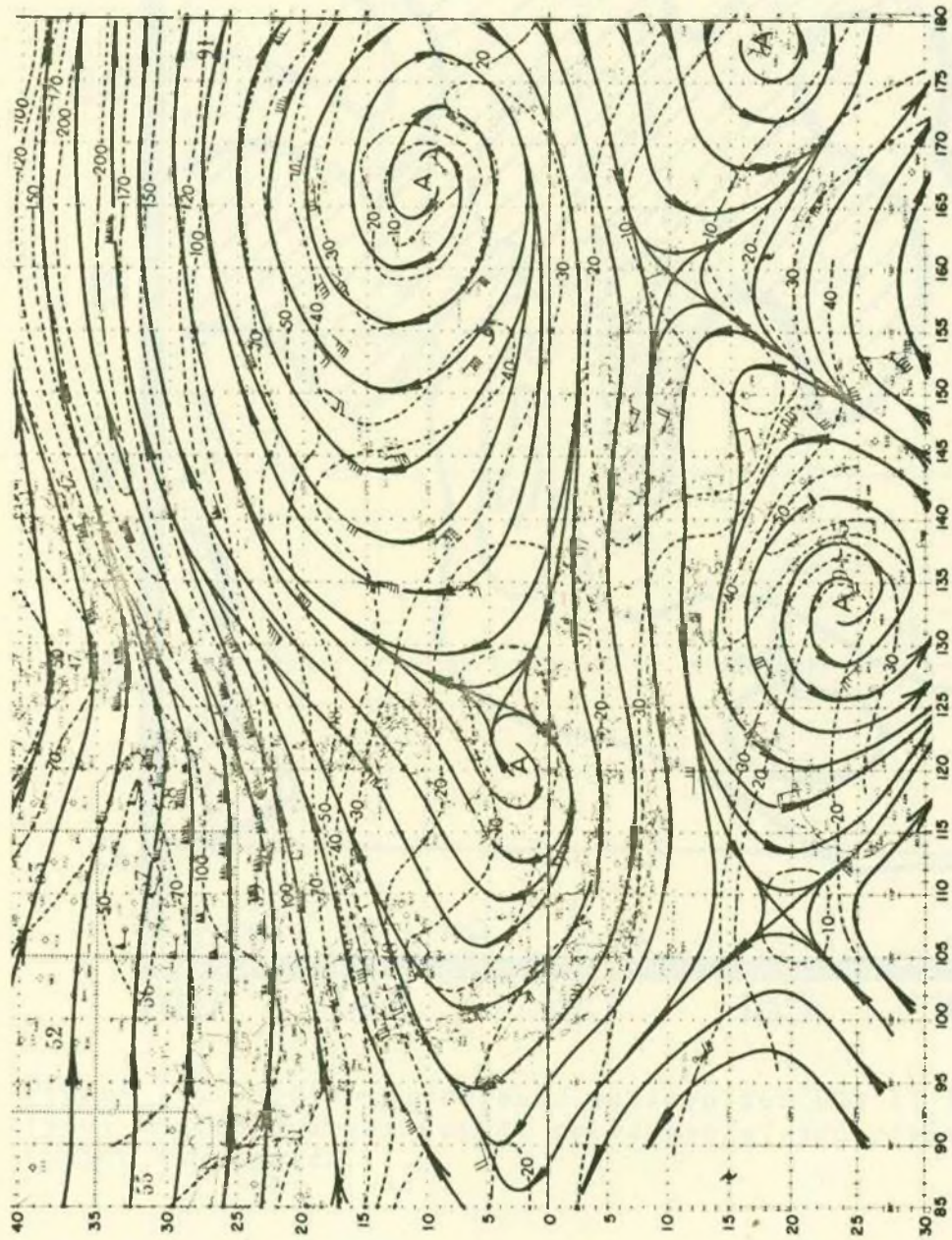


Figure 16. 250 mb streamline and isotach analysis for 00Z 17 February 1970. Streamlines are full, and isotachs are dashed (knots).

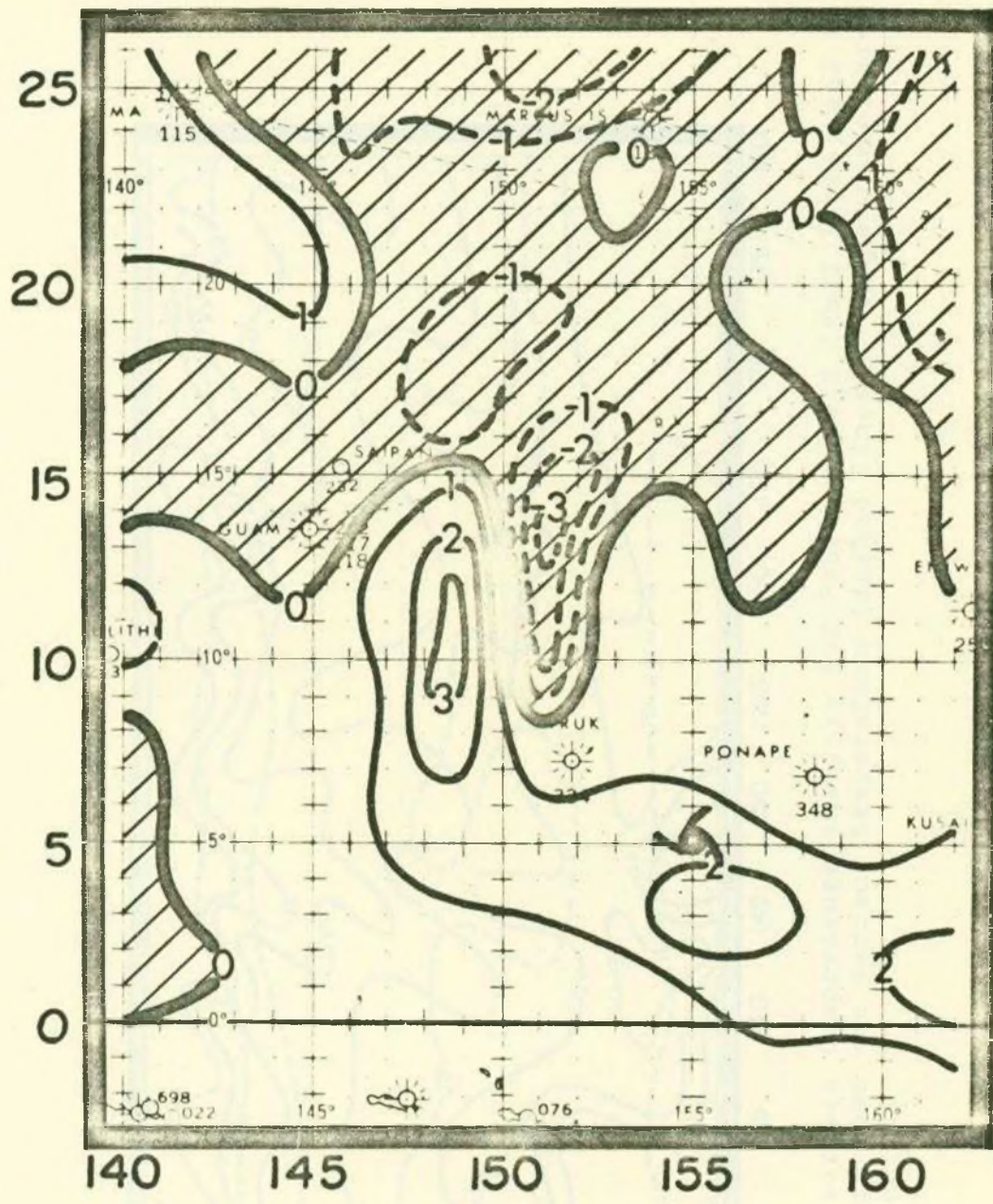


Figure 17. 250 mb divergence pattern for 00Z 17 February 1970. Hatched areas depict convergence, and clear areas depict divergence.

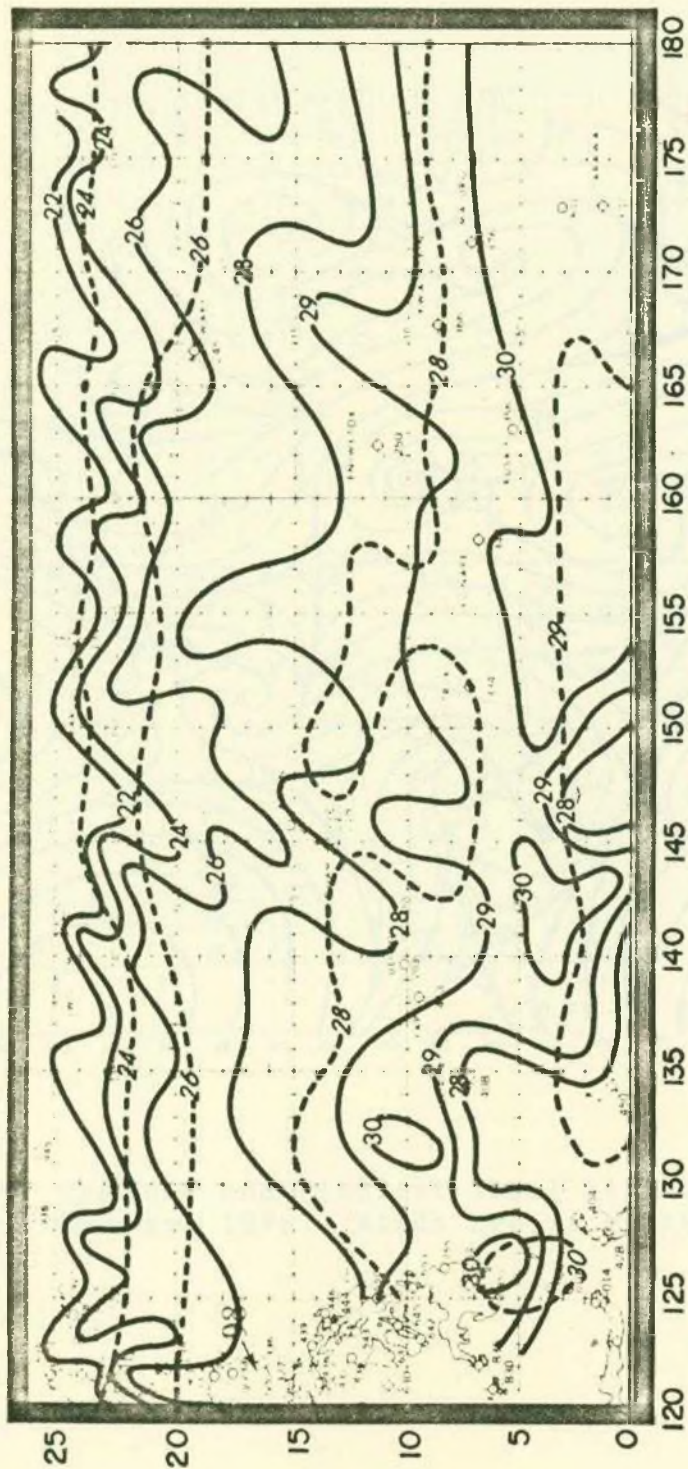


Figure 18. Sea surface temperature analysis for February 1970 (full lines) and the February long term mean sea surface temperature (dashed lines). Temperatures are in degrees Centigrade.

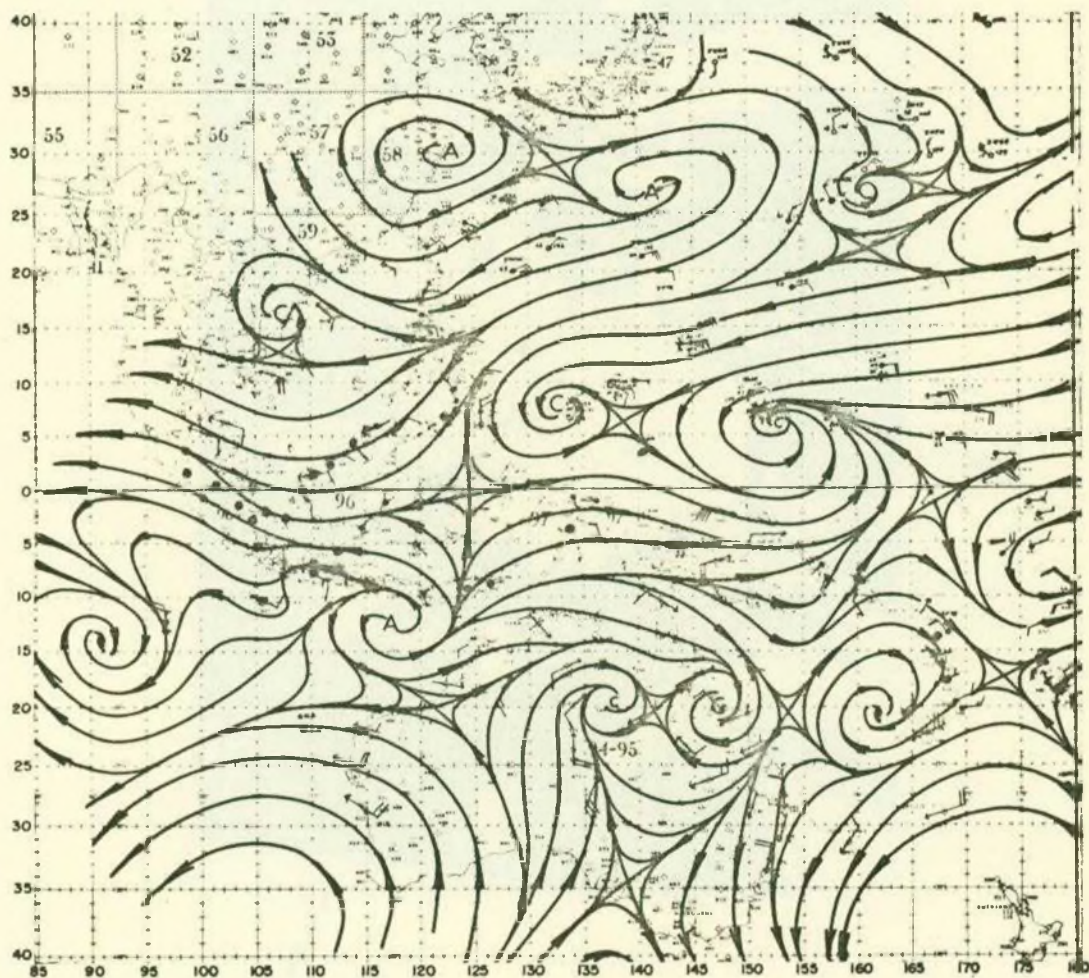


Figure 19. Surface and gradient level streamline analysis for 00Z 18 February 1970. Winds are in knots.

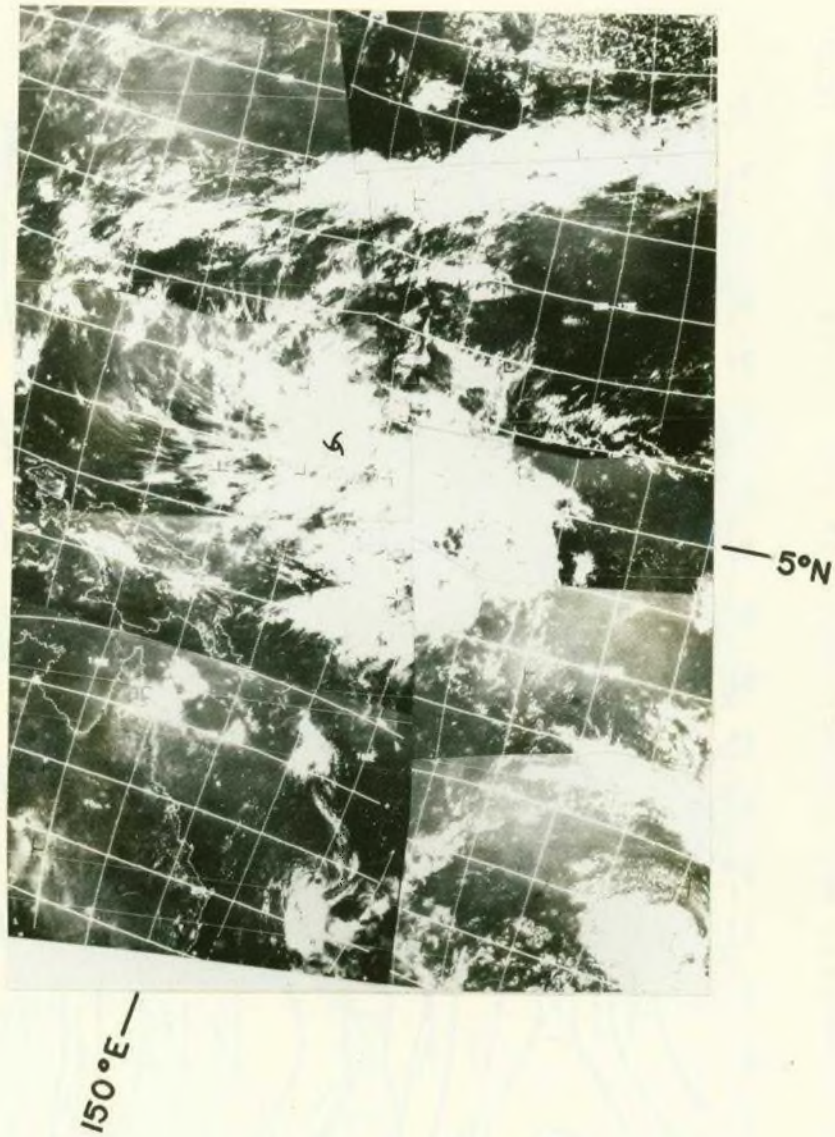


Figure 20. ESSA 9 satellite orbital composite photograph for 18 February 1970.

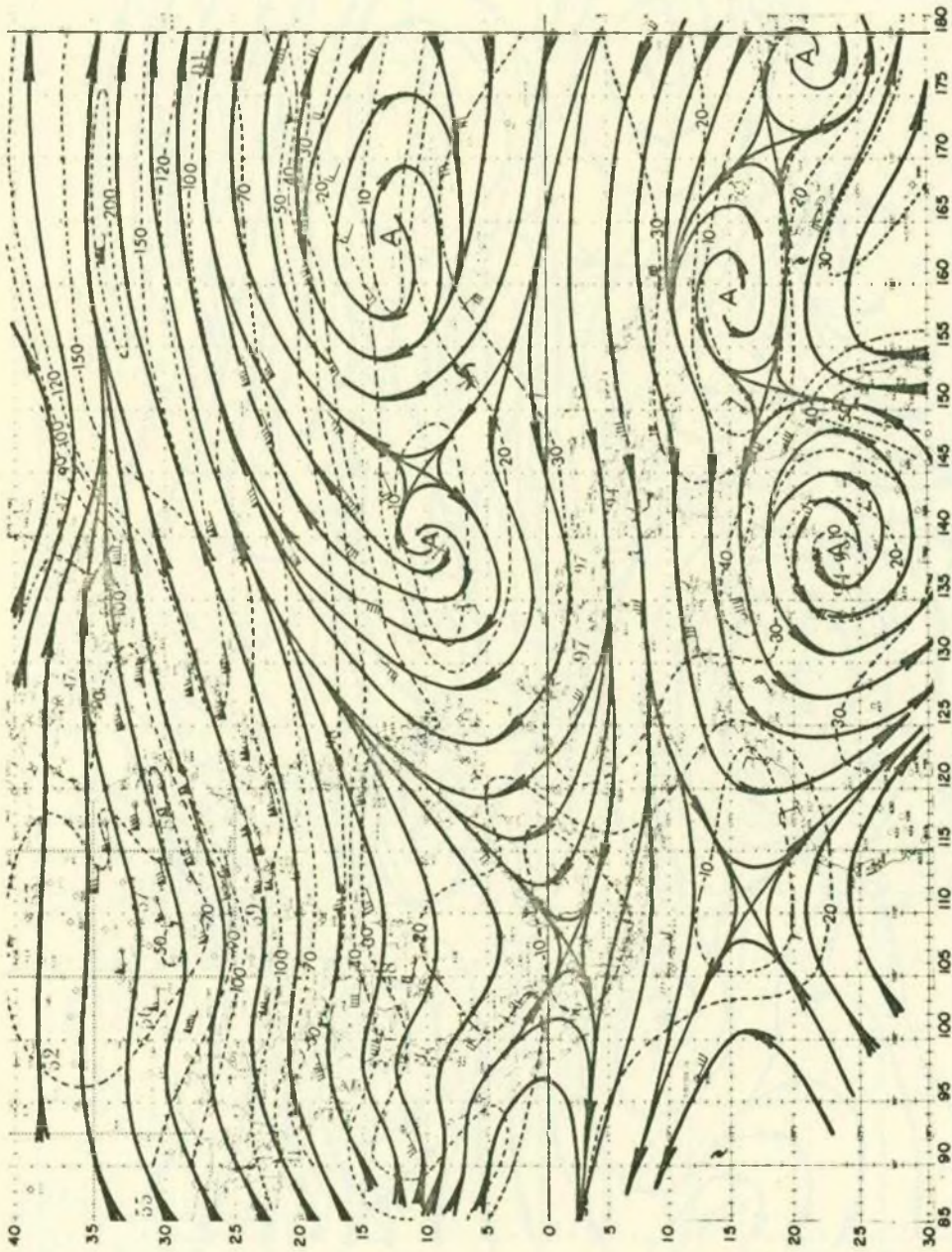


Figure 21. 250 mb streamline and isotach analysis for 00Z 18 February 1970. Streamlines are full, and isotachs are dashed (knots).



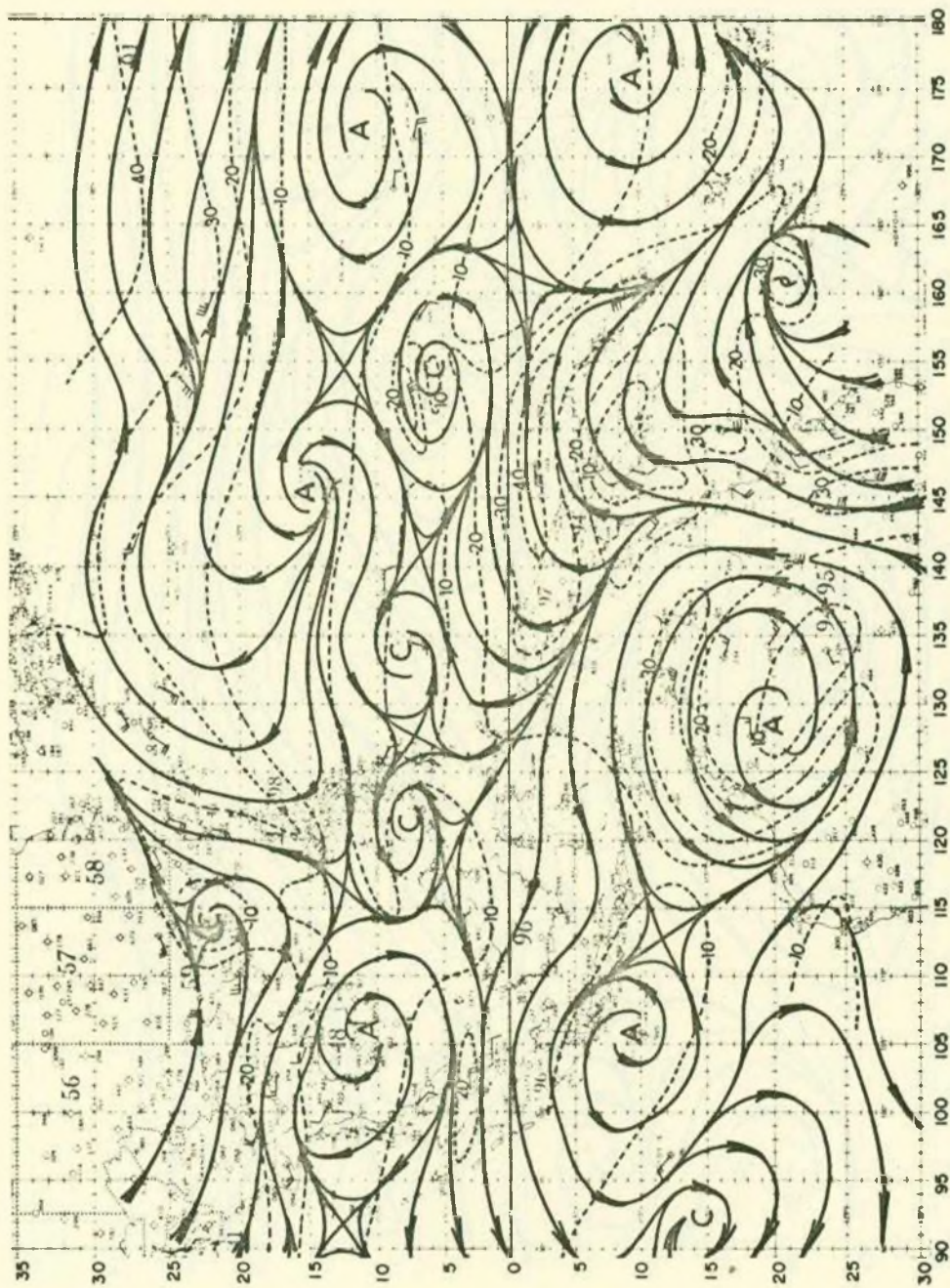


Figure 22. 700 mb streamline and isotach analysis for 00Z 18 February 1970. Streamlines are full, and isotachs are dashed (knots).

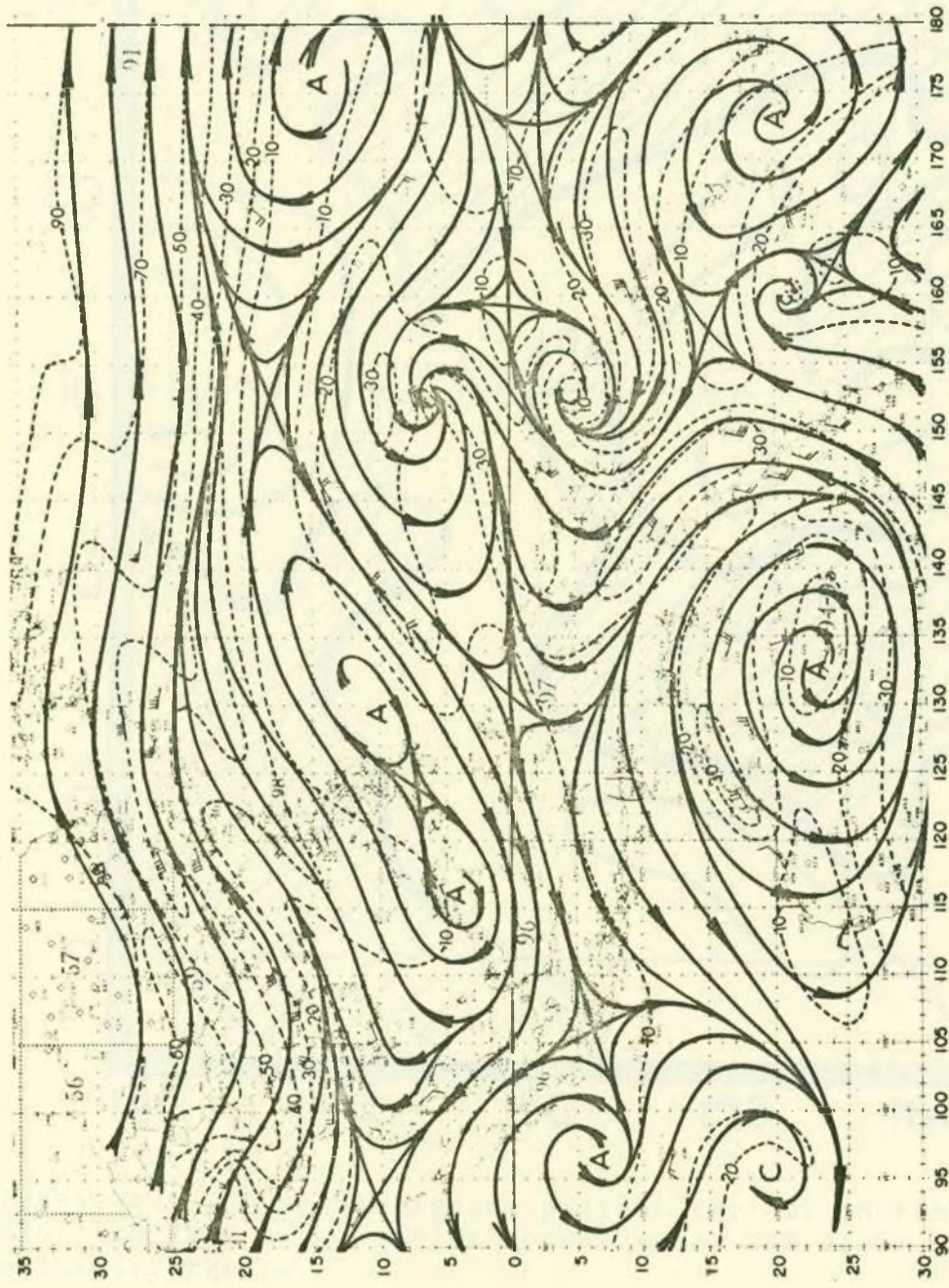


Figure 23. 500 mb streamline and isotach analysis for 00Z 18 February 1970. Streamlines are full, and isotachs are dashed (knots).

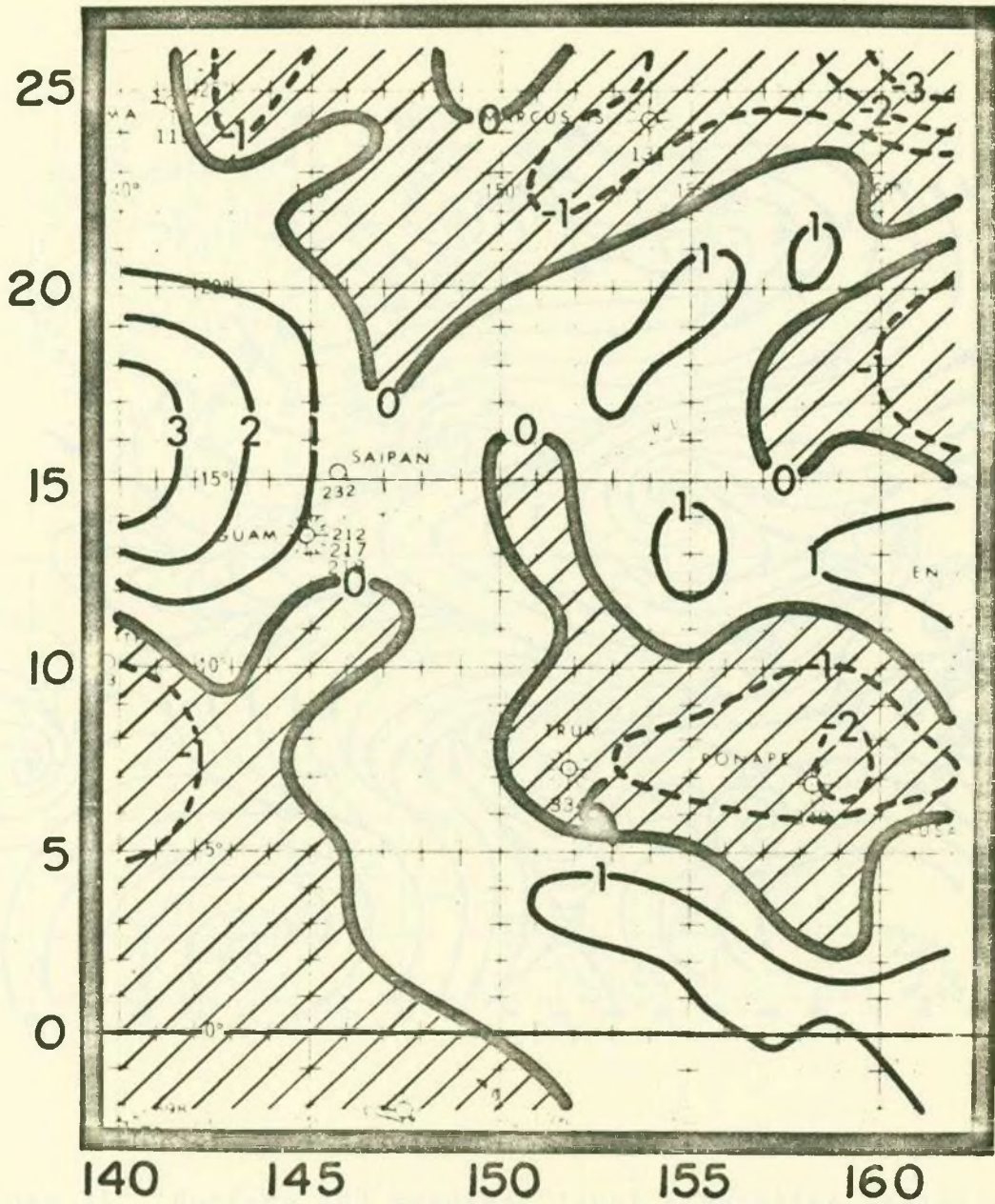


Figure 24. 250 mb divergence pattern for 00Z 18 February 1970. Hatched areas depict convergence, and clear areas depict divergence.

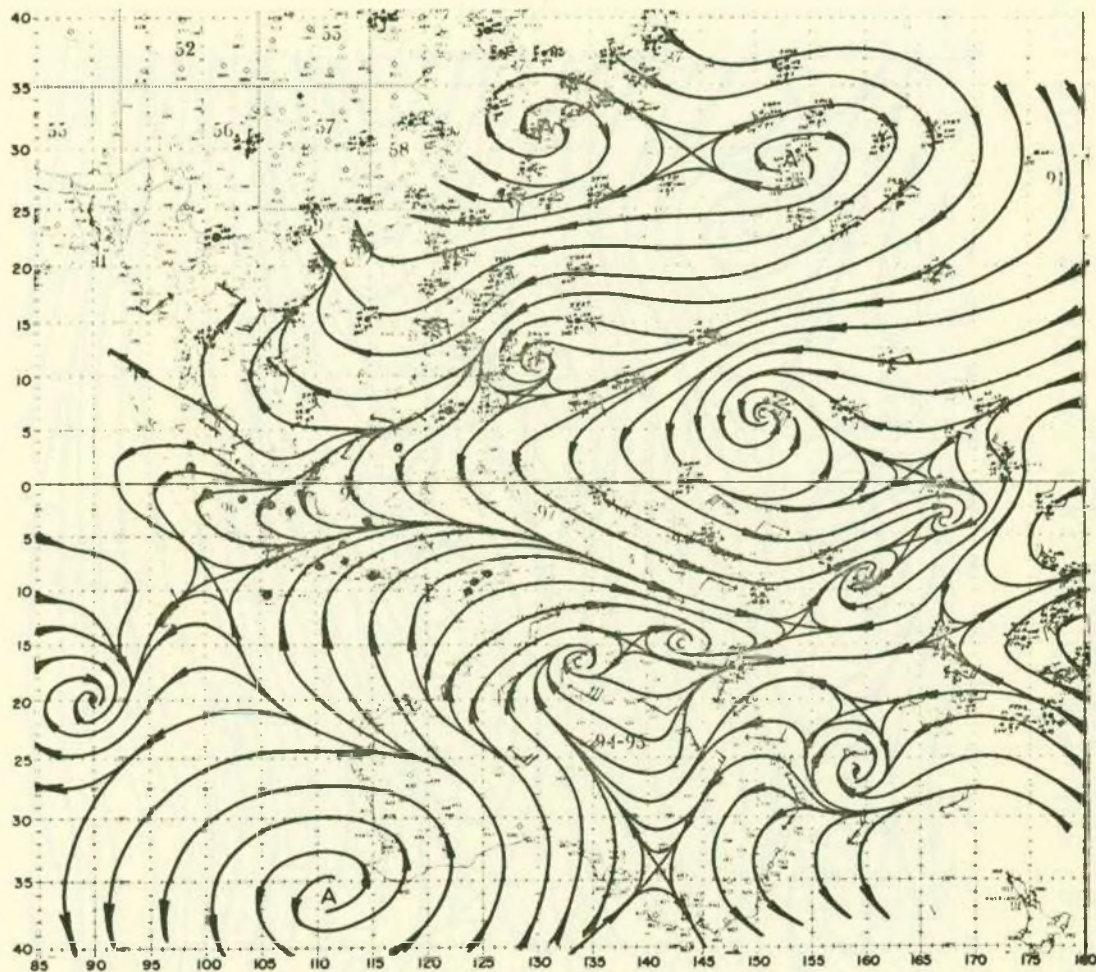


Figure 25. Surface and gradient level streamline analysis for 00Z 19 February 1970. Winds are in knots.

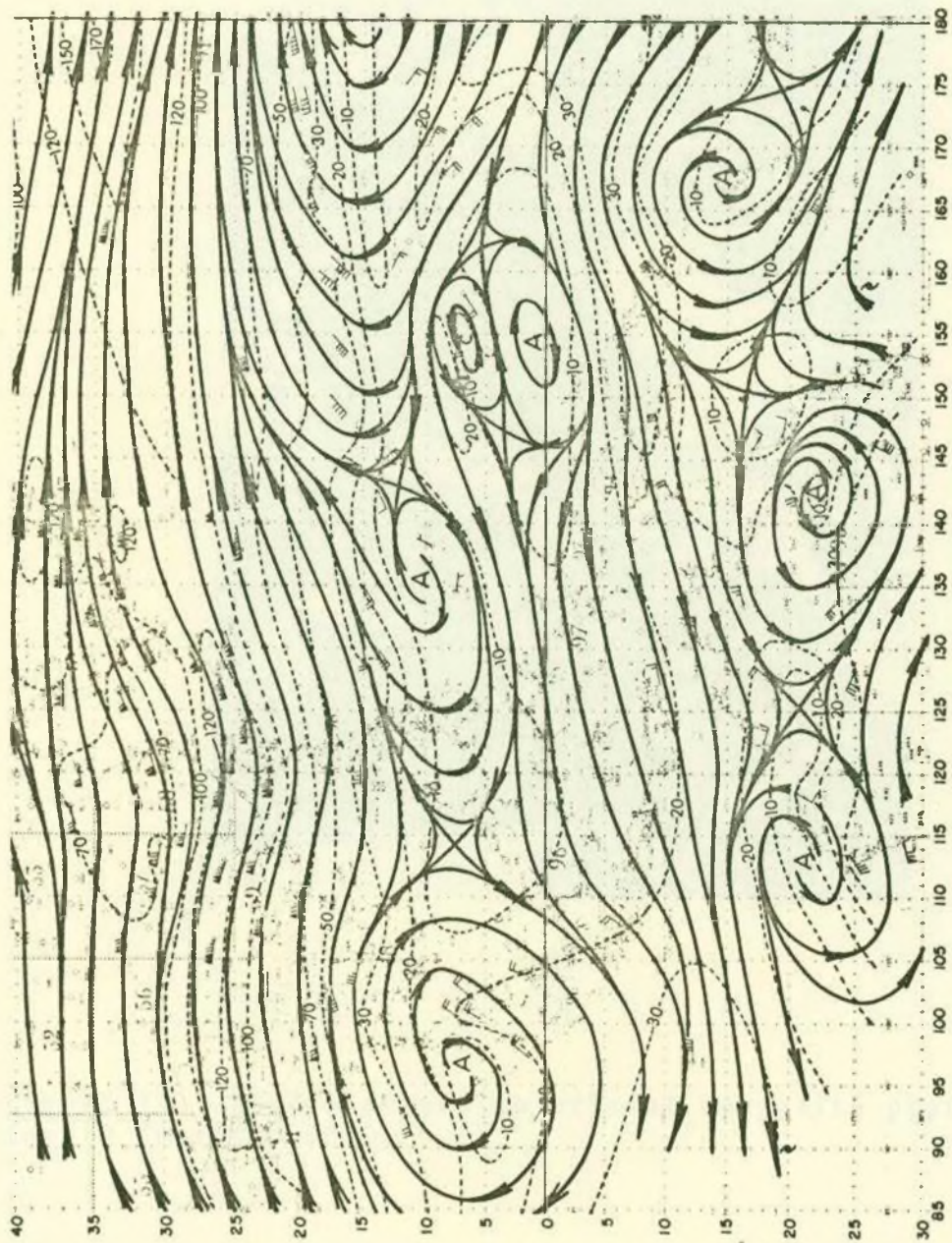


Figure 26. 250 mb streamline and isotach analysis for 00Z 19 February 1970. Streamlines are full, and isotachs are dashed (knots).

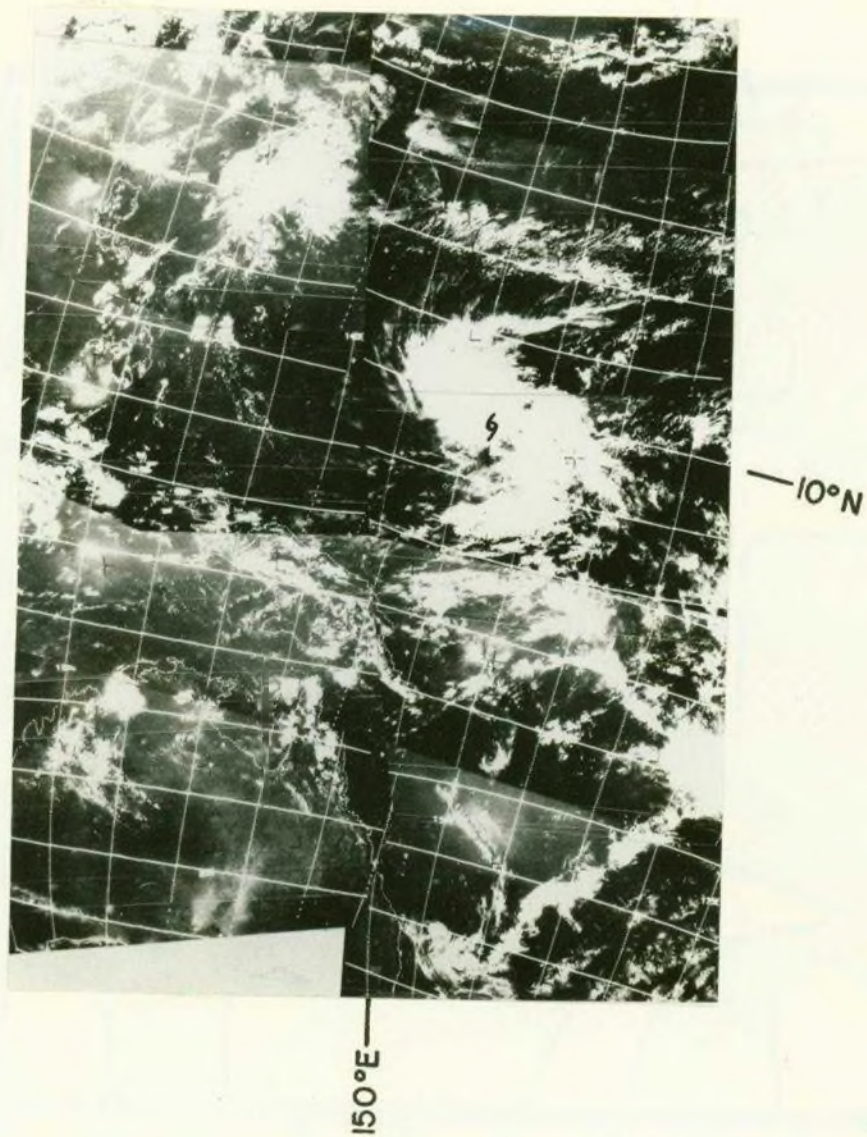


Figure 27. ESSA 9 satellite orbital composite photograph for 19 February 1970.

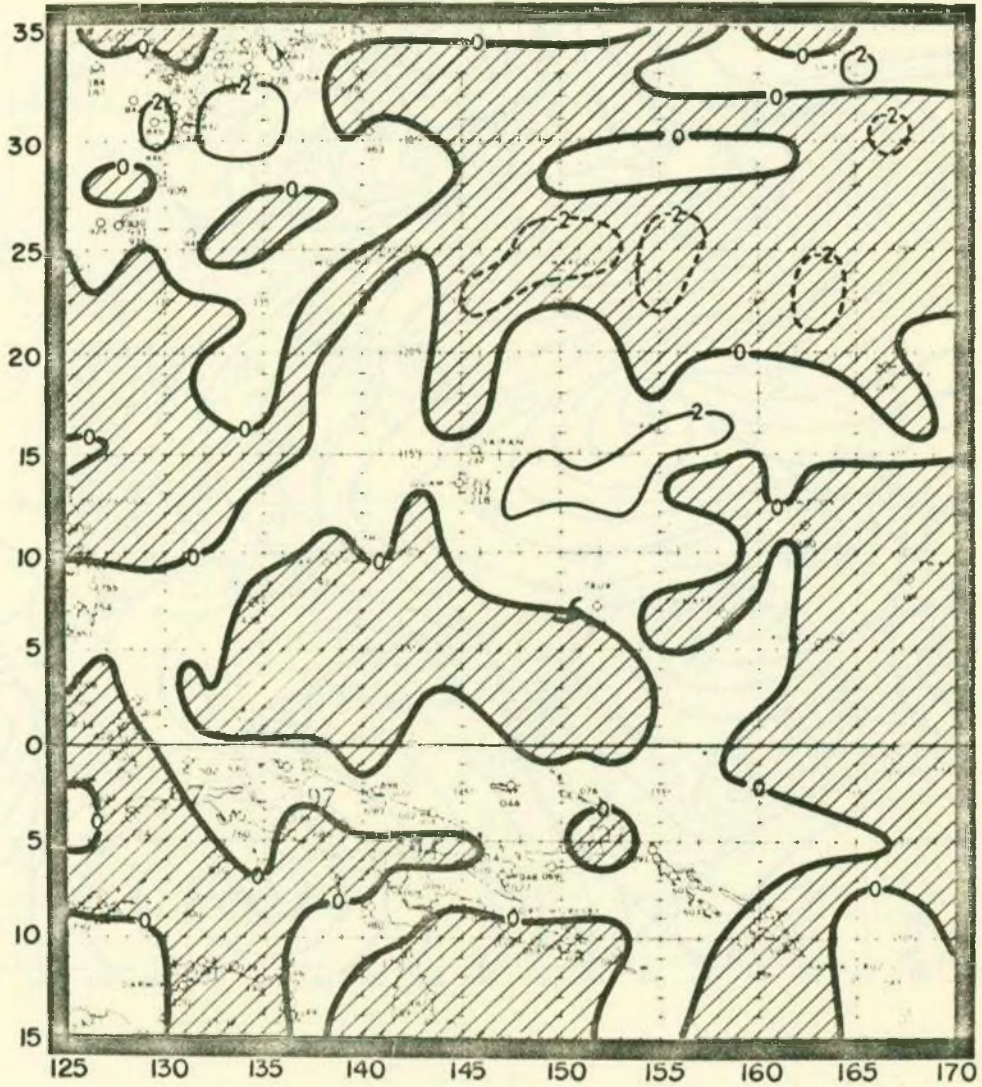


Figure 28. 250 mb divergence pattern for 00Z 19 February 1970. Hatched areas depict convergence, and clear areas depict divergence.

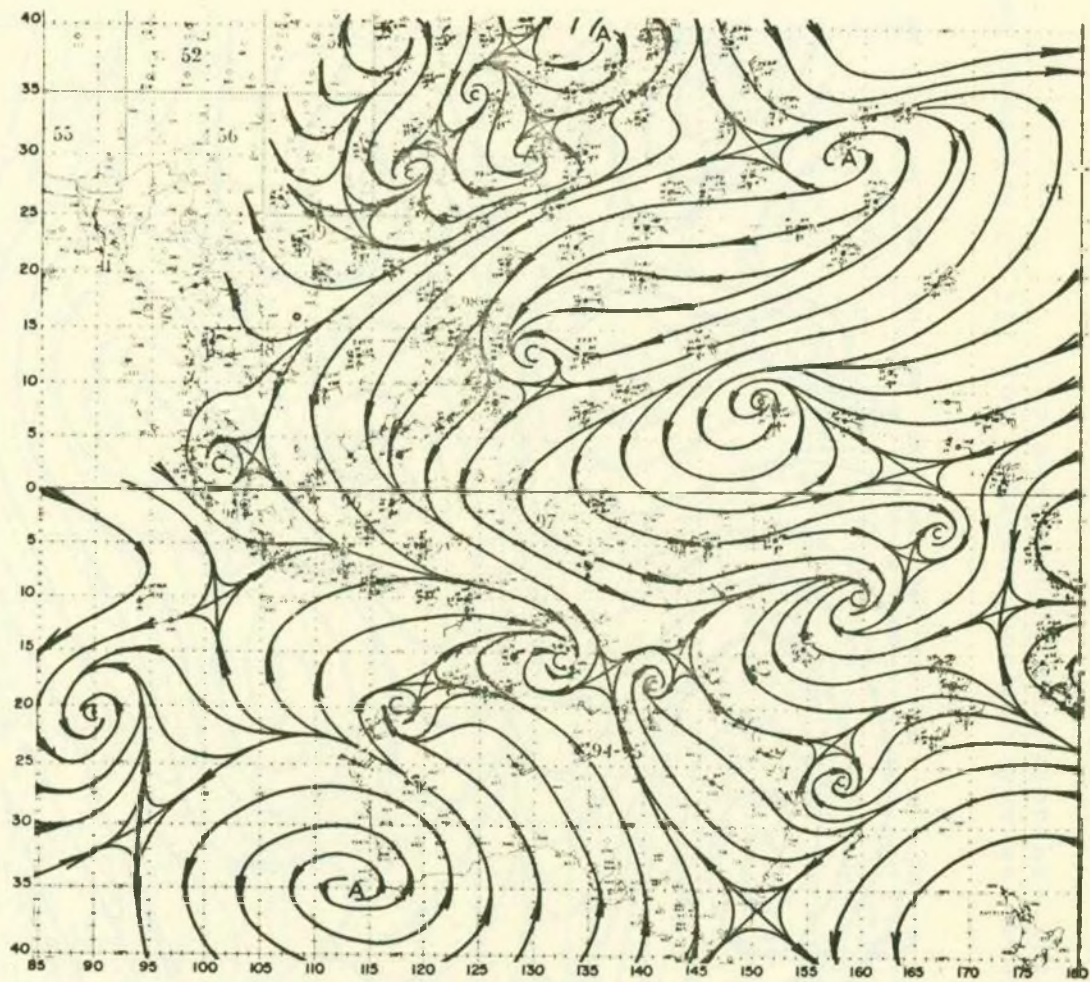


Figure 29. Surface and gradient level streamline analysis for 12Z 19 February 1970. Winds are in knots.



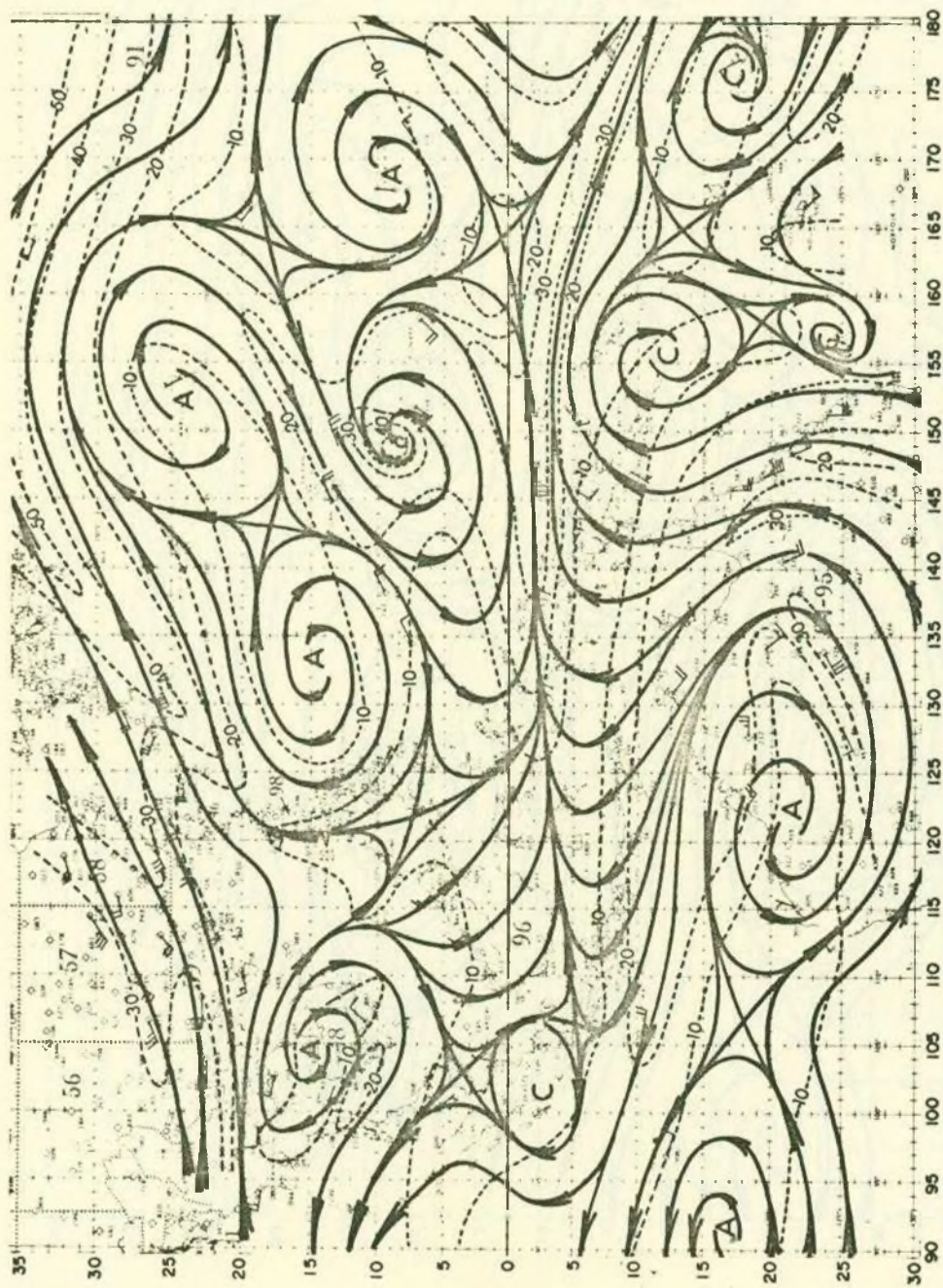


Figure 30. 700 mb streamline and isotach analysis for 12Z 19 February 1970. Streamlines are full, and isotachs are dashed (knots).

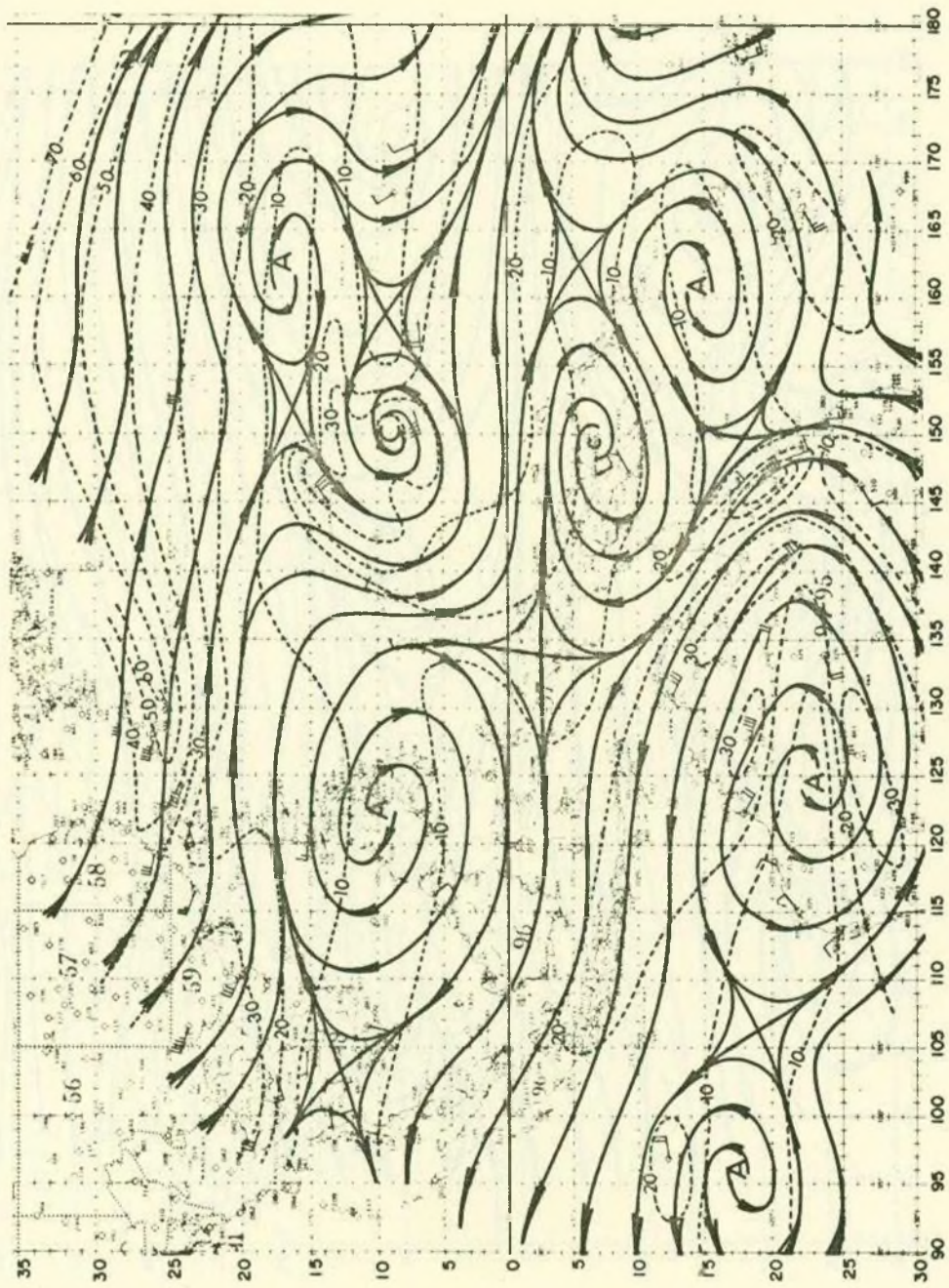


Figure 31. 500 mb streamline and isotach analysis for 12Z 19 February 1970. Streamlines are full, and isotachs are dashed (knots).

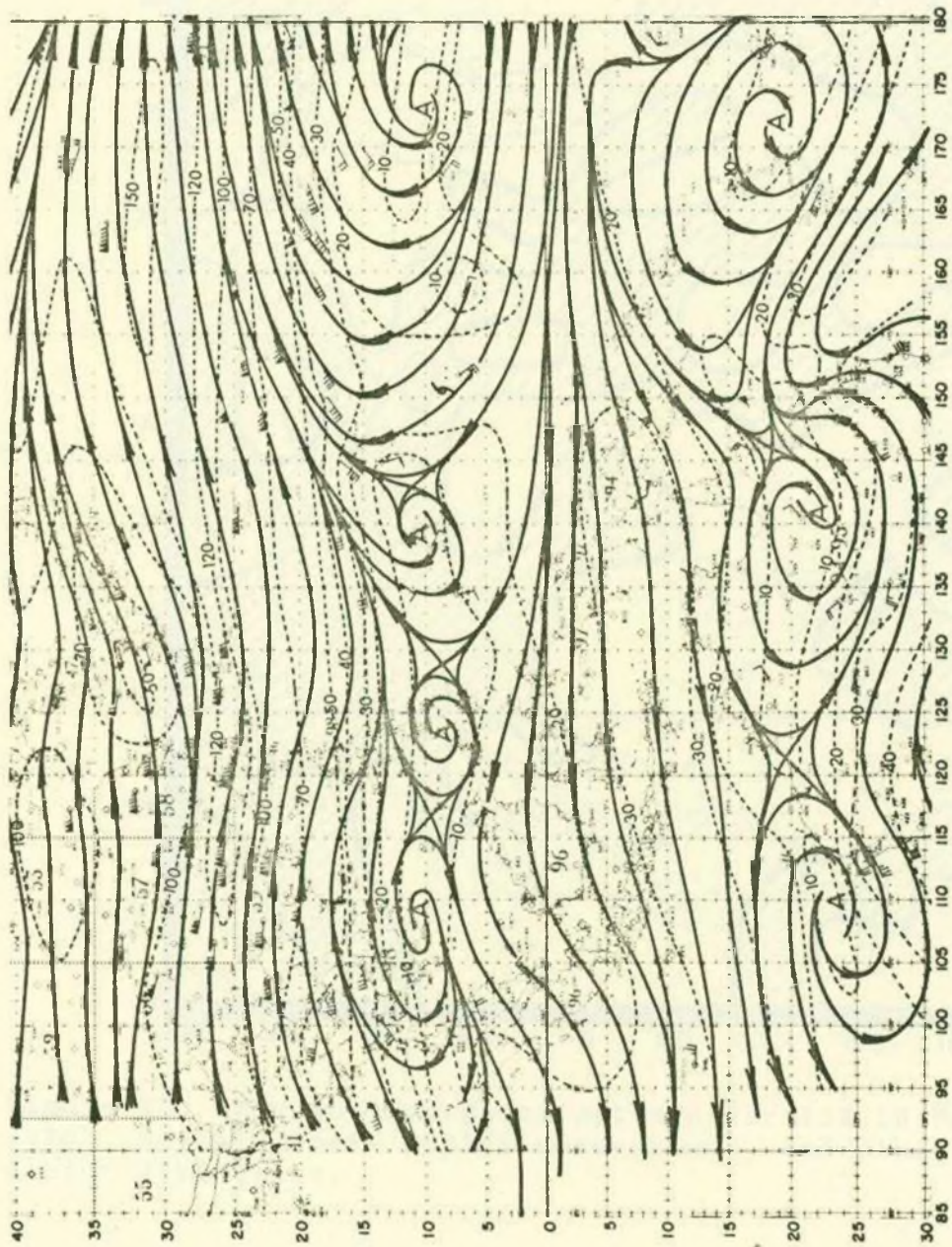


Figure 32. 250 mb streamline and isotach analysis for 12Z 19 February 1970. Streamlines are full, and isotachs are dashed (knots).

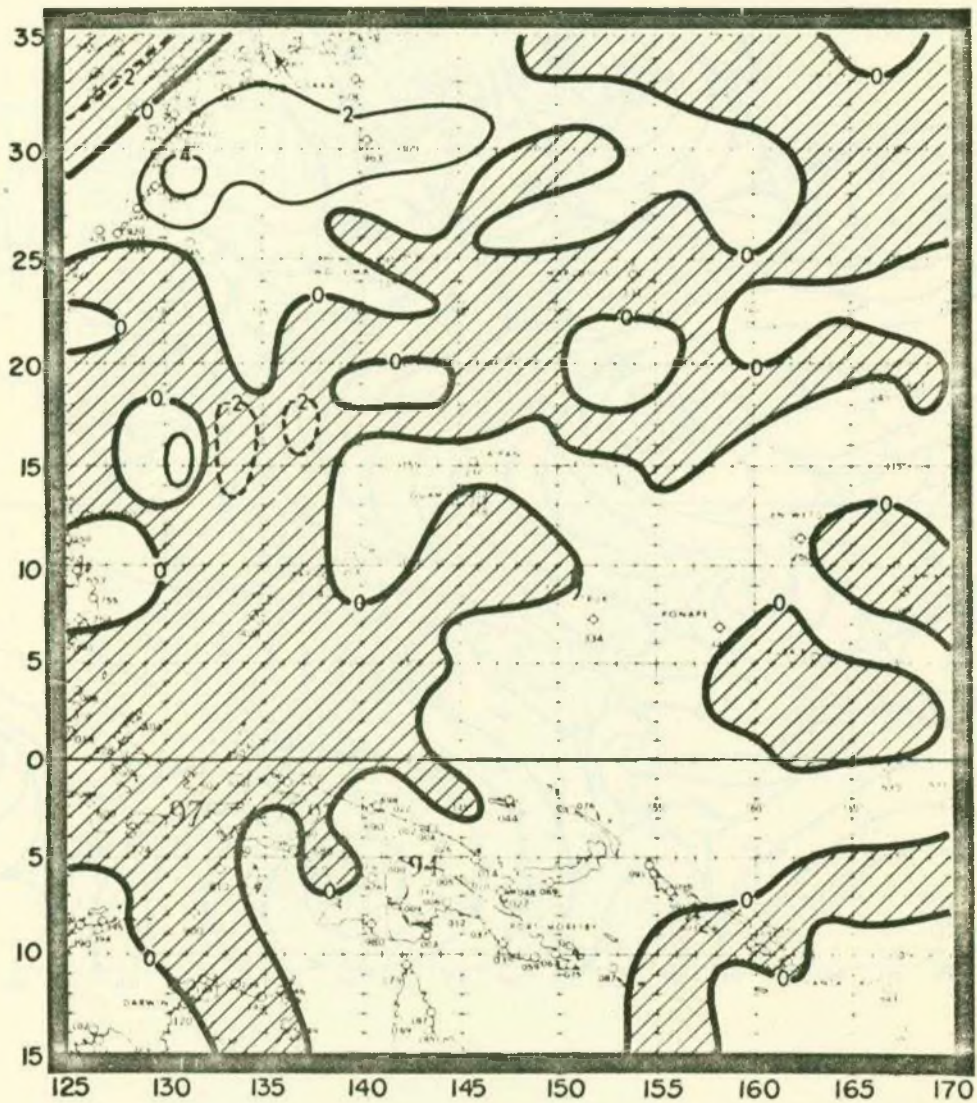


Figure 33. 250 mb divergence pattern for 12Z 19 February 1970. Hatched areas depict convergence, and clear areas depict divergence.

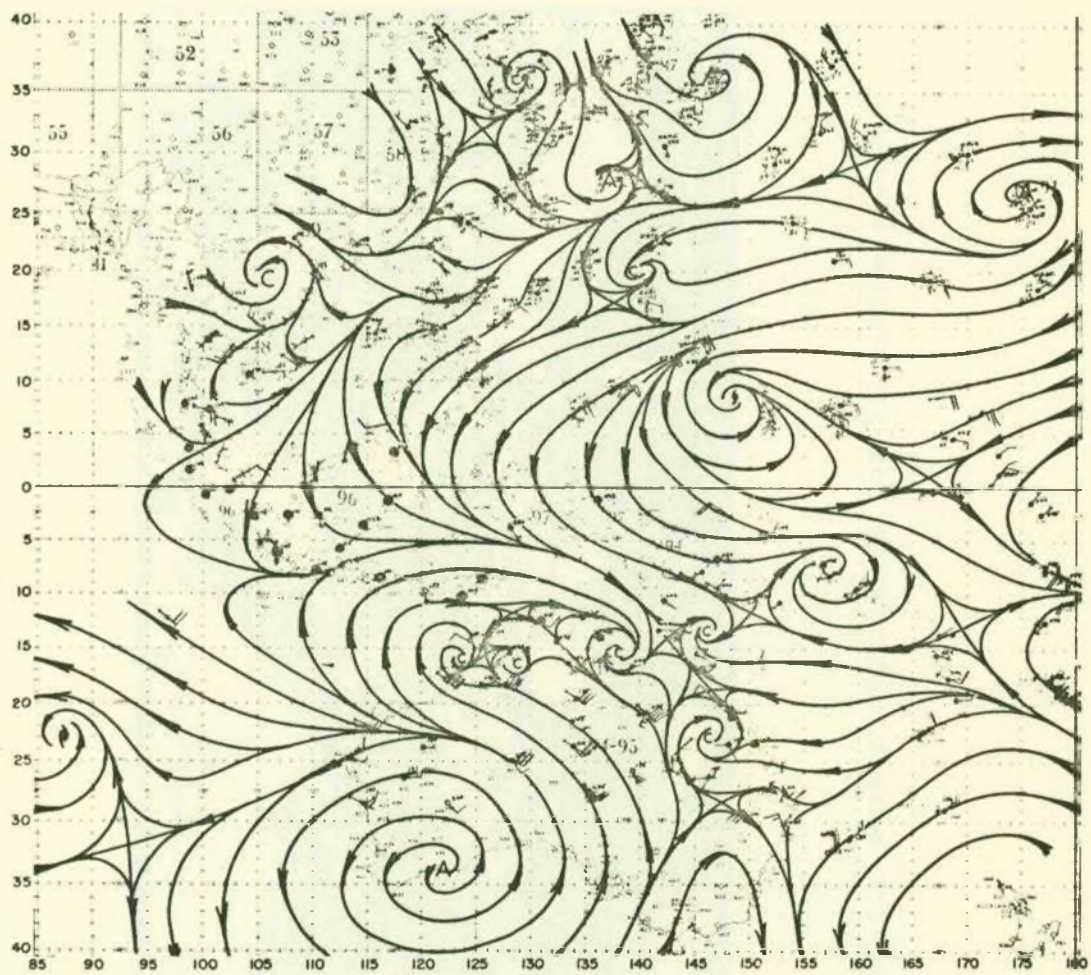


Figure 34. Surface and gradient level streamline analysis for 00Z 20 February 1970. Winds are in knots.

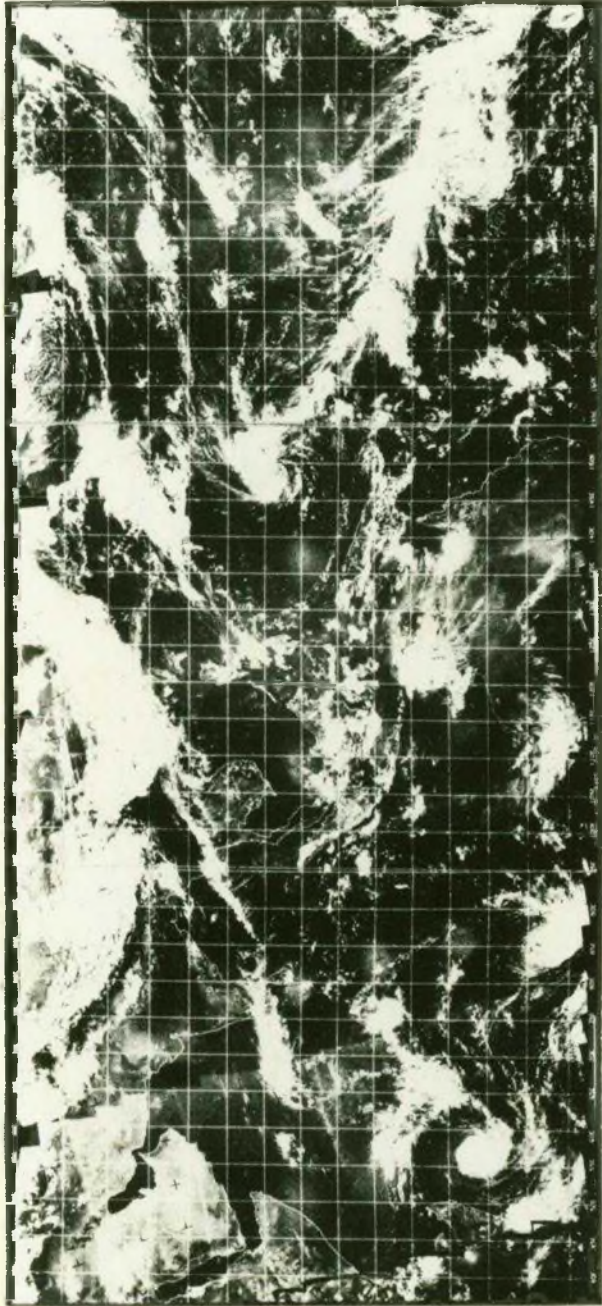


Figure 35. ESSA 9 satellite mosaic photograph for 20 February 1970.

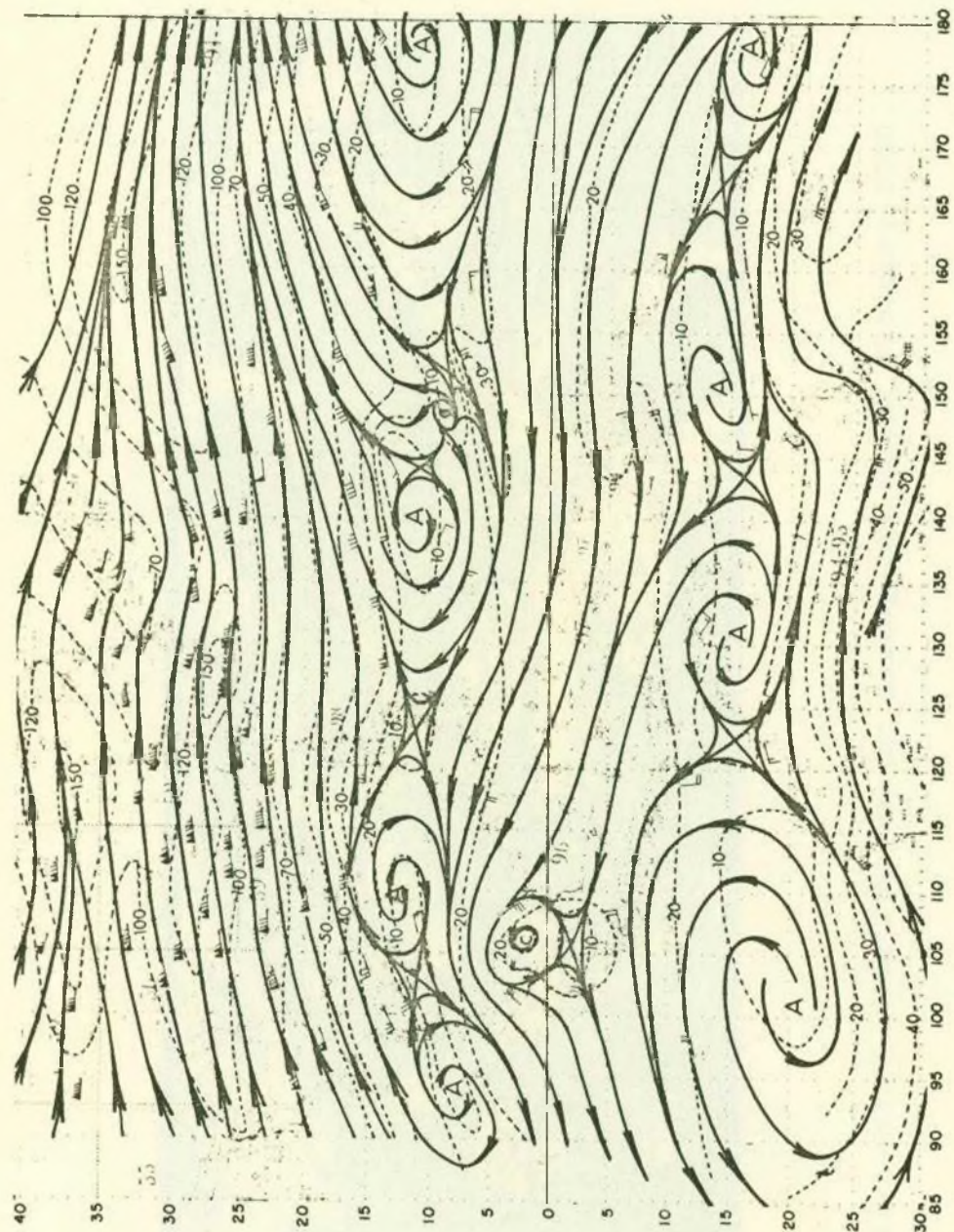


Figure 36. 250 mb streamline and isotach analysis for 00Z 20 February 1970. Streamlines are full, and isotachs are dashed (knots).

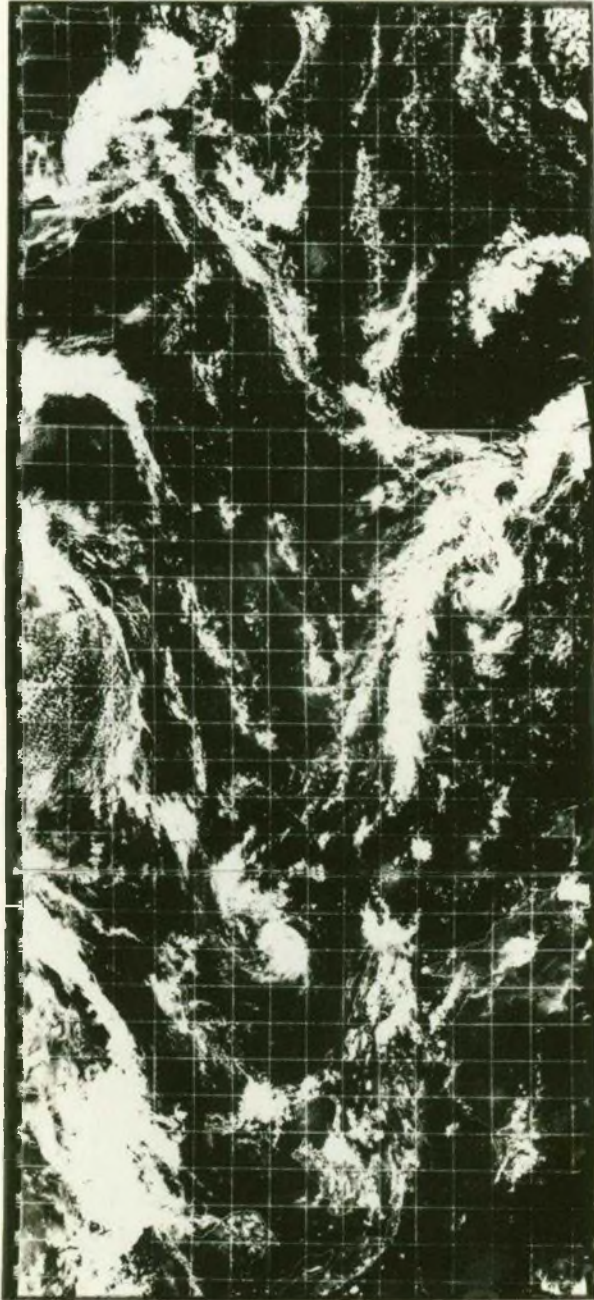


Figure 37. ESSA 9 satellite mosaic photograph for 21 February 1970.



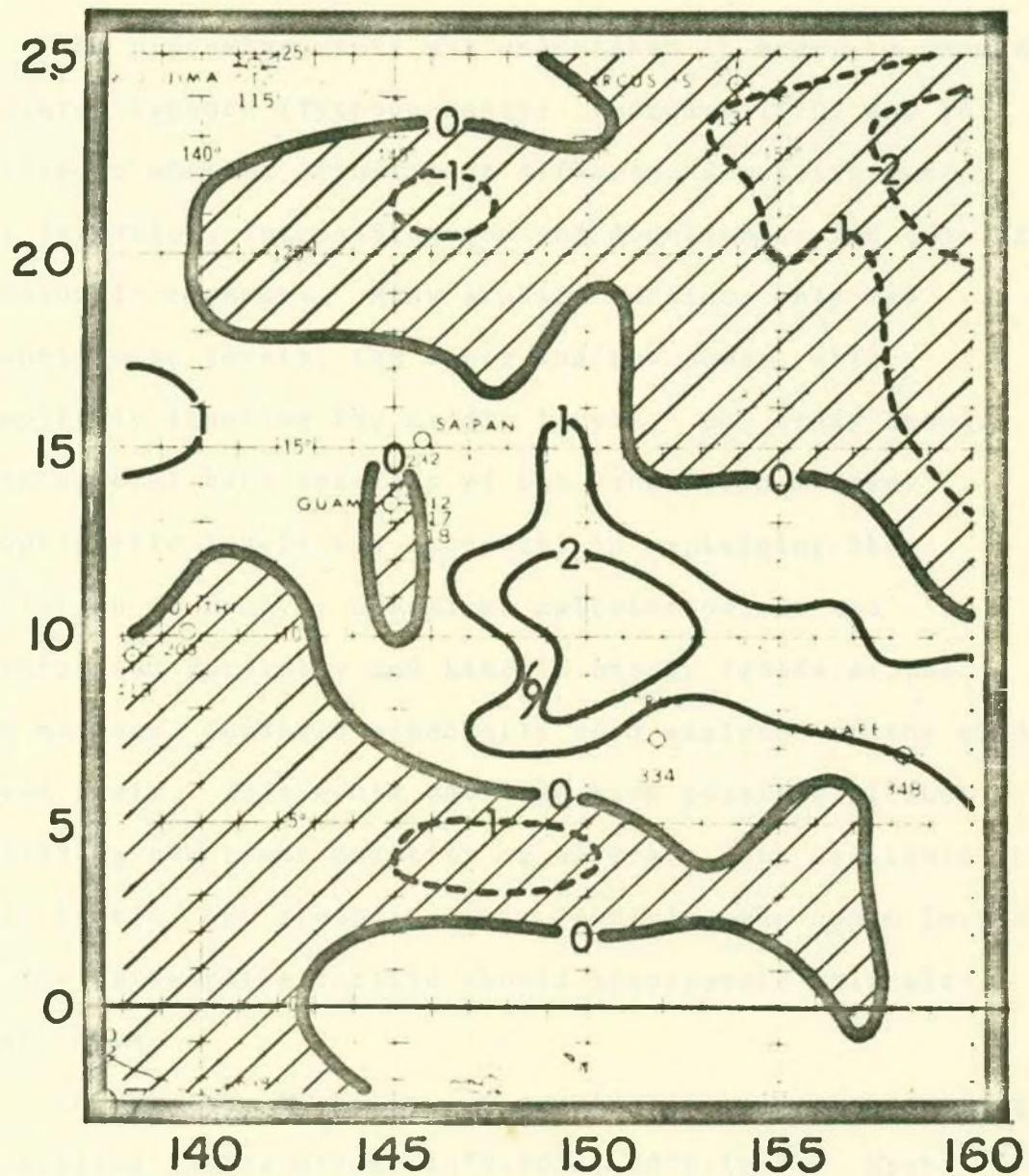


Figure 38. 250 mb divergence pattern for 00Z 20 February 1970. Hatched areas depict convergence, and clear areas depict divergence.

### 3.0. SOME SUGGESTIONS FOR FURTHER RESEARCH

The preceding study was undertaken in order to examine a winter typhoon (Typhoon Nancy: February 1970) and to determine whether significant differences exist between her formation, intensification and development and that of "seasonal" typhoons. Many studies consider only two tropospheric levels, the upper and the lower, while completely ignoring the middle levels. Our study showed that careful hand analyses of the wind field at many tropospheric levels was essential in explaining the evolution of Nancy. Dynamical calculations of the divergence, vorticity and kinetic energy fields at the 250 mb level demanded especially good analyses of the wind speed field. This would not have been possible without utilizing the great quantity of aircraft data available at this level. Any synoptic study involving the upper levels of the data-sparse Pacific should incorporate this aircraft data.

In the case of Nancy, we considered an area exceeding 20 million square miles ( $40^{\circ}\text{N}$ - $30^{\circ}\text{S}$ ,  $90^{\circ}\text{E}$ - $180^{\circ}$ ). Most studies of tropical cyclones consider only the immediate environment of the storm. Such a study of Nancy would have revealed few, if any, differences between her formation, intensification and development and that of "seasonal" tropical cyclones.

We showed that the evolution of Typhoon Nancy was involved with significant changes in the general circulation at all levels. Further studies involving "off-season typhoons" (possibly statistical) need to be performed to determine the frequency of association between strong upper level local increases in wind speed and: (1) local increases in convective activity; (2) occurrences of tropical disturbances, depressions and cyclones; and (3) strong low level local increases in wind speed.

The study suggests that the rareness of "off-season typhoons" is, in part, a result of the normal absence of two probably interdependent situations during the winter months: (1) a sea surface temperature maximum in the region of formation and (2) westerly winds along and north of the equator. To further verify these observations, two studies must be performed: one assessing the sea surface temperature distribution during periods when winter tropical cyclones occur; and another assessing the existence of westerly winds north of the equator prior to formation of the initial vortex.

Finally, it was shown that large fluxes of moisture may play a significant role in intensifying low pressure areas which later develop into tropical depressions or larger circulations. All case studies of tropical cyclones should, in the future, consider this effect on the earliest stages of the storm.

## REFERENCES

- Bhumralkar, C. M. (1974). Effect of moisture on the hydrostatic pressure. J. Appl. Meteor., 13, 174-175.
- Burroughs, L. D. (1974). Autumnal Tropical-Subtropical Interaction in the Atmosphere over the Western North Pacific and the South China Sea. Unpublished thesis. University of Hawaii.
- Byers, H. R. (1944). General Meteorology. (1937), 2 ed., New York, McGraw-Hill, 645 pp.
- Deppermann, C. E. (1941). On the occurrence of dry stable maritime air in the equatorial regions. Bull. Amer. Meteor. Soc., 22, 143-149.
- Gibbs, W. J. (1956). Two cases of cyclogenesis in tropical latitudes. Trop. Cyclone Symp., Brisbane, December 1956. Bureau of Meteorology, Melbourne, Australia, 275-288.
- Gray, W. M. (1968). Global view of the origin of tropical disturbances and storms. Mon. Wea. Rev., 96, 669-700.
- Holton, J. R. (1972). Introduction to Dynamical Meteorology. New York, Academic Press, 319 pp.
- Johnson, D. H. and H. T. Mörth (1960). Forecasting research in East Africa. Tropical Meteorology in Africa. Nairobi, Munitalp Foundation, 446 pp.
- Koteswaram, P. and C. A. George (1957). The formation and structure of tropical cyclones in the Indian Sea areas. J. Meteor. Soc. Japan, 75, 309-322.
- Malkus, J. S. and H. Riehl (1960). On the dynamics and energy transformations in steady-state hurricanes. Tellus, 12, 1-20.
- McRae, J. N. (1956). The formation and development of tropical cyclones during the 1955-56 season in Australia. Trop. Cyclone Symp., Brisbane, December 1956. Bureau of Meteorology, Melbourne, Australia, 233-261.
- Miller, B. I. (1958). The three dimensional wind structure around a tropical cyclone. National Hurricane Res. Project Rep. No. 15.

- Murakami, T. and J. C. Sadler (1973). On the fluctuations of the mid-Pacific trough during the early summer of 1971. Contribution No. 73-10, Department of Meteorology, University of Hawaii. (Submitted to J. Atmos. Sci.)
- Namias, J. (1955). Long range factors affecting the genesis and paths of tropical cyclones. Proc. UNESCO Symp. Typhoons, Tokyo, November 9-12, 1954, 213-219.
- Palmer, C. E. (1951). Tropical meteorology. Compendium of Meteorology. Boston, A.M.S., 859-880.
- Palmer, C. E. (1952). Tropical meteorology. Quart. J. Roy. Meteor. Soc., 78, 126-164.
- Palmén, E. (1956). Formation and development of tropical cyclones. Trop. Cyclone Symp., Brisbane, December 1956. Bureau of Meteorology, Melbourne, Australia, 213-231.
- Palmén, E. and C. W. Newton (1969). Atmospheric Circulation Systems Their Structure and Interpretation. New York, Academic Press, 603 pp.
- Ramage, C. S. (1959). Hurricane development. J. Meteor., 16, 227-237.
- Ramage, C. S. (1971). Monsoon Meteorology. New York, Academic Press, 296 pp.
- Ramage, C. S. (1973). The typhoons of October 1970 in the South China Sea: intensification, decay and ocean interaction. ENVPREDRSCHFAC Tech. Paper No. 4-73 and UHMET 72-05, 41 pp.
- Ramage, C. S. (1974). Monsoonal influences on the annual variation in tropical cyclone development. Presented at A.M.S. National Meeting, Honolulu, HI, January 8-11 of 1974. (in preparation for publication)
- Riehl, H. (1945). Waves in the easterlies and the polar front in the tropics. Misc. Rep. No. 17, University of Chicago.
- Riehl, H. (1948). On the formation of typhoons. J. Meteor., 5, 247-264.
- Riehl, H. (1954). Tropical Meteorology. New York, McGraw-Hill, 392 pp.

- Sadler, J. C. (1967). On the origin of tropical vortices. Proc. of Working Panel on Trop. Dyn. Meteor., August 1967. Navy Weather Research Facility, Norfolk, VA, 39-75.
- Sutrisno, C. (1963). The effect of tropical cyclones in the western North Pacific and the Bay of Bengal on the weather in the southwestern part of Indonesia. Proc. of Symp. of Trop. Meteor., Rotorua, New Zealand. New Zealand Meteorological Service, Wellington, NZ, 201-215.
- Wilkie, W. R. (1964). Evaluation of methods of forecasting development and movement of cyclones in the Northeast Australian Region. Proc. of Symp. of Trop. Meteor., Rotorua, New Zealand. New Zealand Meteorological Service, Wellington, NZ, 715-729.

## DATA SOURCES

- Bureau of Meteorology, Monthly Climate Data--Surface Australia. February 1970. Melbourne, Victoria, Australia.
- Bureau of Meteorology, Monthly Climate Data--Upper Air Australia. February 1970. Melbourne, Victoria, Australia.
- Environmental Technical Applications Center, Surface weather data. February 1970. Washington, D. C.
- Environmental Technical Applications Center, Upper air data. February 1970. Washington, D. C.
- Fleet Numerical Weather Central, Atlas of Monthly Mean Sea Surface Temperature and Depth of the Top of the Thermocline, North Pacific Ocean. May 1971. Monterey, California.
- Fleet Numerical Weather Central, 6 hourly 200, 250, and 300 mb plotreps. February 1970. Pearl Harbor, Hawaii.
- Fleet Numerical Weather Central, 6 hourly 700 mb plotreps. February 1970. Pearl Harbor, Hawaii.
- Japan Meteorological Agency (1970). Aerological Data of Japan February 1970. Tokyo, Japan.
- Japan Meteorological Agency, Daily Weather Maps. Vol. 45, February 1970. Tokyo, Japan.
- Meteorological Services Malaysia, Pilot Balloon and Radar Wind Data. February 1970. Kuala Lumpur, Malaysia.
- National Environmental Satellite Service, ESSA 9 Satellite Photographs, Tracks 7 & 8. February 16-19, 1970. Suitland, Maryland.
- National Environmental Satellite Service, ESSA 9 Satellite Mosaic Photographs. February 1970. Suitland, Maryland.
- National Weather Service, Northern Hemisphere Data Collection. February 1970. Asheville, North Carolina.

- New Zealand Meteorological Service, Daily Weather Bulletins. February 1970. Wellington, New Zealand.
- Nouvelle-Caledonie et Dependances, Resume Mensuel Du Temps. February 1970. Noumea, New Caledonia.
- Philippine Weather Bureau, Observational Results: Surface Marine Observations. February 1970. Quezon City, Republic of the Philippines.
- Ramage, C. S. and C. V. R. Raman (1972). Meteorological Atlas of the International Indian Ocean Expedition--Upper Air, Vol. 2. Washington, D. C., National Science Foundation.
- Republic of Viet Nam, Upper Air Soundings. February 1970. Saigon, Viet Nam.
- Regional Meteorological Center, Darwin, Daily Weather Maps, (surface and 700, 500, 300, 200 mb levels). February 1970. Darwin, Northern Territory, Australia.
- United Kingdom, Air Ministry Meteorological Office, Daily Upper Air Analyses. February 1970. Singapore.
- United Kingdom, Air Ministry Meteorological Office, Ship Weather Report Log Book. February 1970. Hong Kong.
- United States Department of Commerce, Environmental Science Services Administration (1967). World Weather Records 1951-1960, Asia. Vol. 4. Washington, D. C.
- United States Department of Commerce, Environmental Science Services Administration (1968). World Weather Records 1951-1960, Antarctica, Australia, Oceanic Islands, and Ocean Weather Stations. Vol. 6. Washington, D. C.
- United States Fleet Weather Central/Joint Typhoon Warning Center (1971). Annual Typhoon Report 1970. Guam, Marianas Islands.